Available online at www.sciencedirect.com
ScienceDirect
Remote Sensing of Environment 106 (2007) 106–122
Remote Sensing of Environment
www.elsevier.com/locate/rse

Canopy spectral invariants for remote sensing and model applications

Dong Huang [a,*], Yuri Knyazikhin [a], Robert E. Dickinson [b], Miina Rautiainen [c], Pauline Stenberg [c], Mathias Disney [d], Philip Lewis [d], Alessandro Cescatti [e,f], Yuhong Tian [b], Wout Verhoef [g], John V. Martonchik [h], Ranga B. Myneni [a]

[a] *Department of Geography, Boston University, 675 Commonwealth Avenue, Boston, MA 02215, USA*
[b] *School of Earth and Atmospheric Sciences, Georgia Institute of Technology, Atlanta, GA, USA*
[c] *Department of Forest Ecology, University of Helsinki, Helsinki, Finland*
[d] *NERC Centre for Terrestrial Carbon Dynamics and Department of Geography, University College London, London, UK*
[e] *Centro di Ecologia Alpina, Viote del Monte Bondone, 38100 Trento, Italy*
[f] *Climate Change Unit, Institute for Environment and Sustainability, European Commission Joint Research Centre, Ispra, Italy*
[g] *National Aerospace Laboratory NLR, Amsterdam, The Netherlands*
[h] *Jet Propulsion Laboratory, California Institute of Technology, Pasadena, CA, USA*

Received 15 May 2006; received in revised form 31 July 2006; accepted 2 August 2006

Abstract

The concept of canopy spectral invariants expresses the observation that simple algebraic combinations of leaf and canopy spectral transmittance and reflectance become wavelength independent and determine a small set of canopy structure specific variables. This set includes the canopy interceptance, the recollision and the escape probabilities. These variables specify an accurate relationship between the spectral response of a vegetation canopy to the incident solar radiation at the leaf and the canopy scale and allow for a simple and accurate parameterization for the partitioning of the incoming radiation into canopy transmission, reflection and absorption at any wavelength in the solar spectrum. This paper presents a solid theoretical basis for spectral invariant relationships reported in literature with an emphasis on their accuracies in describing the shortwave radiative properties of the three-dimensional vegetation canopies. The analysis of data on leaf and canopy spectral transmittance and reflectance collected during the international field campaign in Flakaliden, Sweden, June 25–July 4, 2002 supports the proposed theory. The results presented here are essential to both modeling and remote sensing communities because they allow the separation of the structural and radiometric components of the measured/modeled signal. The canopy spectral invariants offer a simple and accurate parameterization for the shortwave radiation block in many global models of climate, hydrology, biogeochemistry, and ecology. In remote sensing applications, the information content of hyperspectral data can be fully exploited if the wavelength-independent variables can be retrieved, for they can be more directly related to structural characteristics of the three-dimensional vegetation canopy.

Keywords: Spectral invariants; Recollision probability; Escape probability; Radiative transfer

1. Introduction

The solar energy that transits through the atmosphere to the vegetation canopy is made available to the atmosphere by reflectance and transformation of radiant energy absorbed by plants and soil into fluxes of sensible and latent heat and thermal radiation through a complicated series of bio-physiological, chemical and physical processes. To quantitatively predict the vegetation and atmospheric interactions and/or to monitor the vegetated Earth from space, therefore, it is important to specify those environmental variables that determine the shortwave energy conservation in vegetation canopies; that is, partitioning of the incoming radiation between canopy absorption, transmission and reflection.

Interaction of solar radiation with the vegetation canopy is described by the three-dimensional radiative transfer equation (Ross, 1981). The interaction cross-section (extinction coefficient) that appears in this equation is treated as wavelength independent considering the size of the scattering elements

* Corresponding author. Tel.: +1 617 353 8846; fax: +1 617 353 8399.
E-mail address: dh@bu.edu (D. Huang).

0034-4257/$ - see front matter © 2006 Elsevier Inc. All rights reserved.
doi:10.1016/j.rse.2006.08.001

(leaves, branches, twigs, etc.) relative to the wavelength of solar radiation (Ross, 1981). Although the scattering and absorption processes are different at different wavelengths, the interaction probabilities for photons in vegetation media are determined by the structure of the canopy rather than photon frequency or the optics of the canopy. This feature results in canopy spectral invariant behaviour for a vegetation canopy bounded from below by a non-reflecting surface; that is, the difference between numbers of photons incident on phytoelements within the vegetation canopy at two arbitrary wavelengths is proportional to the difference between numbers of photons scattered by phytoelements at the same wavelengths (Knyazikhin et al., 1998, 2005) and is purely a function of canopy structural arrangement. A wavelength-independent coefficient of proportionality is the probability that a photon scattered from a phytoelement will interact within the canopy again—the recollision probability (Smolander & Stenberg, 2005). The canopy interceptance, defined as the probability that a photon from solar radiation incident on the vegetation canopy will hit a leaf, is another wavelength-independent variable (Smolander & Stenberg, 2005) which is directly derivable from the canopy spectral invariant. The canopy spectral absorptance is an explicit function of the wavelength-independent recollision probability and canopy interceptance, and wavelength-dependent absorptance of an average leaf. These three variables, recollision probability, canopy interceptance and leaf absorptance, therefore, determine the partitioning of the top of canopy radiation into its absorbed and canopy leaving portions.

The spectral invariant relationships have also been reported for canopy transmittance (Panferov et al., 2001; Shabanov et al., 2003) and reflectance (Disney et al., 2005; Lewis et al., 2005), suggesting that the canopy leaving radiation can further be broken down into its reflected and transmitted portions. Wang et al. (2003) hypothesize that a small set of independent variables that appear in the spectral invariant relationships suffice to fully describe the law of energy conservation in vegetation canopies at any wavelength in the solar spectrum. Such a result is essential to both modeling and remote sensing communities as it allows the measured and modelled canopy signal to be decomposed into structurally varying and spectrally invariant components. The former are a function of canopy age, density and arrangement while the latter are a function of canopy biochemical behaviour. Consequently, the canopy spectral invariants offer a simple and accurate parameterization for the shortwave radiation block in many global models of climate, hydrology, biogeochemistry, and ecology (Bonan et al., 2002; Dickinson et al., 1986; Potter et al., 1993; Raich et al., 1991; Running & Hunt, 1993; Saich et al., 2003; Sellers et al., 1986). For example, Buermann et al. (2001) reported that a more realistic partitioning of incoming solar radiation between the canopy and the ground below the canopy in the NCAR Community Climate Model 3 (Kiehl et al., 1996, 1998) results in improved model predictions of near-surface climate.

In remote sensing applications, the information content of hyperspectral data can be fully exploited if the wavelength-independent variables can be retrieved, for they can be more directly related to structural characteristics of the vegetation canopy. For example, both the recollision probability and the leaf area index (LAI) can be derived from hyperspectral data (Wang et al., 2003). At a given effective LAI, the recollision probability of the coniferous canopy is larger than its leaf canopy counterpart due to within-shoot photon multiple interactions (Smolander & Stenberg, 2005). The recollision probability combined with the LAI, therefore, has a potential to discriminate between broadleaf and coniferous canopies. Such canopy spectral invariant relationships have been exploited in developing algorithms for retrieving LAI and fraction of absorbed photosynthetically active radiation (FPAR) from satellite data of varying spectral band composition and spatial resolution (Tian et al., 2003).

Smolander and Stenberg (2005), however, question the validity of the spectral invariant for canopy transmittance. They

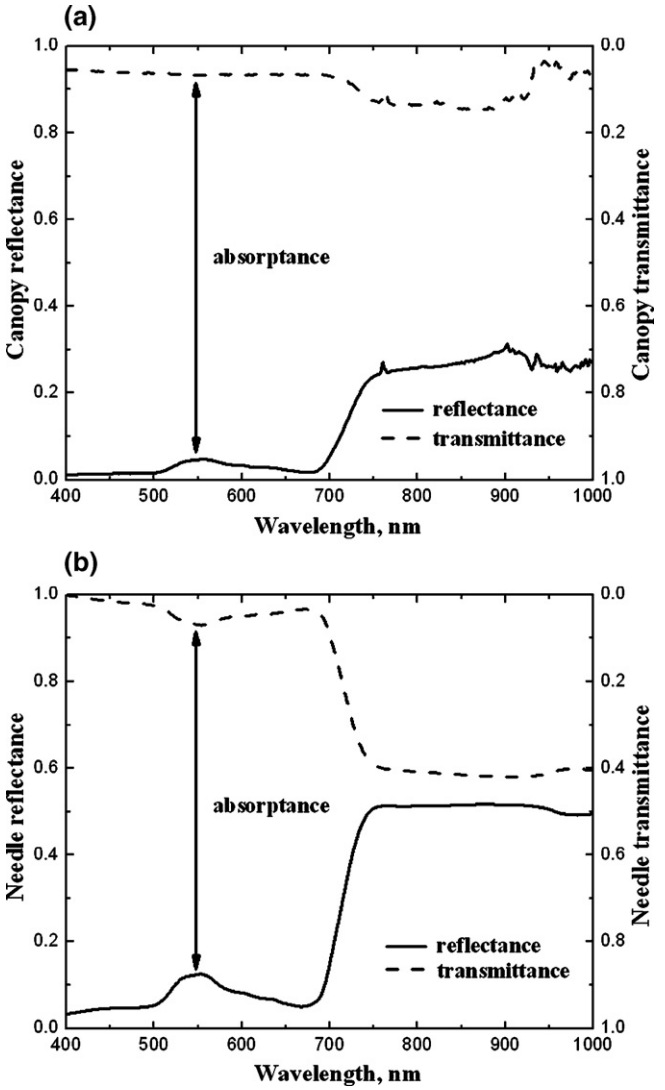

Fig. 1. Canopy (panel a) and needle (panel b) spectral reflectance (vertical axis on the left side) and transmittance (vertical axis on the right side) for a Norway spruce (*P. abies* (L.) Karst) stand. Arrows show needle and canopy absorptance. The needle transmittance and albedo follow the regression line $\tau_L = 0.47\omega - 0.02$ with $R^2 = 0.999$ and RMSE = 0.004. Measurements were taken during an international field campaign in Flakaliden, Sweden, June 25–July 4, 2002 (WWW1, 2002).

show that while the recollision probability and canopy interceptance perform well in estimating the spectral absorption of both homogeneous leaf and shoot canopies, a proposed structural parameter for separation of downward portion of the canopy leaving radiation (Knyazikhin et al., 1998; Panferov et al., 2001; Shabanov et al., 2003) can fail to predict spectral transmittance of the coniferous canopy and spectral transmittance of the leaf canopy at high LAI values. Panferov et al. (2001) suggest that the spectral invariant relationship is not valid for canopy reflectance while Lewis et al. (2003, 2005) and Disney et al. (2005) have demonstrated its validity to describe the transformation for leaf absorptance spectrum to canopy spectral reflectance. The lack of physically based definitions of wavelength-independent variables that determine separation of the down- and upward portions of the canopy leaving radiation is responsible for these conflicting results (Smolander & Stenberg, 2005). The aim of the present paper is to provide a solid theoretical basis for canopy spectral invariants. More specifically, it addresses the following three questions. (i) How can the wavelength-independent structural parameters be defined to achieve an accurate and consistent parameterization for canopy spectral response to the incident solar radiation? (ii) How is the recollision probability related to the wavelength-independent variables that control up- and downward portions of the canopy leaving radiation? Finally, (iii) How accurate are these spectral invariant relationships?

The paper is organized as follows. Canopy spectral invariant relationships reported in the literature are analyzed with data from an international field campaign in a coniferous forest near Flakaliden, Sweden, in Section 2 and Appendix A. Expansion of the 3D radiation field in the successive order of scattering, or Neumann series, and its properties are discussed in Section 3 and Appendix B. Spectral invariants for canopy interaction coefficients, reflectance, transmittance and bidirectional reflectance factors and their accuracies are studied in Sections 4–6. Simplified spectral invariant relationships for use in remote sensing and model studies are analyzed in Section 7. Finally, Section 8 summarizes the results.

2. Canopy spectral invariants: observations

The aim of this section is to illustrate the canopy spectral invariant relationships reported in the literature and to introduce their basic properties using field data collected during an international field campaign in Flakaliden, Sweden, June 25–July 4, 2002. A description of instrumentation, measurement approach and data processing is given in Appendix A.1. It should be noted that the spectral invariant is formulated for a vegetation canopy bounded from below by a non-reflecting surface. However, we will use measured spectra without correcting for canopy substrate effects (i.e., the fact that observed canopies do not have totally absorbing lower boundaries). The impact of surface reflection on canopy reflectance, absorptance and transmittance is discussed in Appendix A.2 and summarized in Fig. A1.

The canopy transmittance (reflectance) is the ratio of the mean downward radiation flux density at the canopy bottom (mean upward radiation flux density at the canopy top) to the downward radiation flux density above the canopy. Similarly, canopy absorptance is the portion of radiation incident on the vegetation canopy that the canopy absorbs. These variables are the three basic components of the law of shortwave energy conservation which describe canopy spectral response to incident solar radiation at the *canopy scale*. If reflectance of the ground below the vegetation is zero, the portion of radiation absorbed, $a(\lambda)$, transmitted, $t(\lambda)$, or reflected, $r(\lambda)$, by the canopy is unity, i.e.,

$$t(\lambda) + r(\lambda) + a(\lambda) = 1. \tag{1}$$

Fig. 1a shows canopy transmittance and reflectance spectra of a 50 m × 50 m plot with planted 40-year-old Norway spruce (Appendix A.1). This plot had been subjected to irrigation and fertilization since 1987. The effective LAI is 4.37.

The leaf transmittance (reflectance) is the portion of radiation flux density incident on the leaf surface that the leaf transmits (reflects). These variables characterize the canopy spectral behavior at the *leaf scale*, are determined by the leaf biochemical constituents, and can vary with tree species, growth conditions, leaf age and their location in the canopy space. The leaf albedo, $\omega(\lambda)$, is the sum of the leaf reflectance, $\rho_L(\lambda)$, and transmittance, $\tau_L(\lambda)$, i.e.,

$$\omega(\lambda) = \rho_L(\lambda) + \tau_L(\lambda). \tag{2}$$

Fig. 1b shows spectral transmittance and reflectance of an average needle derived from the Flakaliden data (Appendix A.1). Measured spectra shown in Fig. 1a and b are used in our examples.

2.1. Canopy spectral invariant for interaction coefficient

The canopy interaction coefficient, $i(\lambda)$, is the ratio of the canopy absorptance $a(\lambda)$ to the absorptance $1-\omega(\lambda)$ of an average leaf (Knyazikhin et al., 2005, p. 633), i.e.,

$$i(\lambda) = \frac{a(\lambda)}{1-\omega(\lambda)} = \frac{1-t(\lambda)-r(\lambda)}{1-\omega(\lambda)}. \tag{3}$$

For a vegetation canopy bounded at its bottom by a black surface, this variable is the mean number of photon interactions with phytoelements at wavelength λ. The portion of photons scattered by leaves is $\omega(\lambda)i(\lambda)$. If $\omega(\lambda)=0$, the canopy interaction coefficient, i_0, is the probability that a photon from the incident radiation will hit a phytoelement—the canopy interceptance (Smolander & Stenberg, 2005). For a vegetation canopy with non-reflecting leaves, the canopy absorptance and interceptance coincide.

Fig. 2a shows the interaction coefficient, $i(\lambda)$, and mean portion of photons scattered by leaves, $\omega(\lambda)i(\lambda)$, as a function of wavelength derived from measured spectra shown in Fig. 1 using Eqs. (2) and (3). The canopy spectral invariant states that the difference, $i(\lambda)-i(\lambda_0)$, between portions of photons incident on phytoelements at two arbitrary wavelengths, λ and λ_0, is

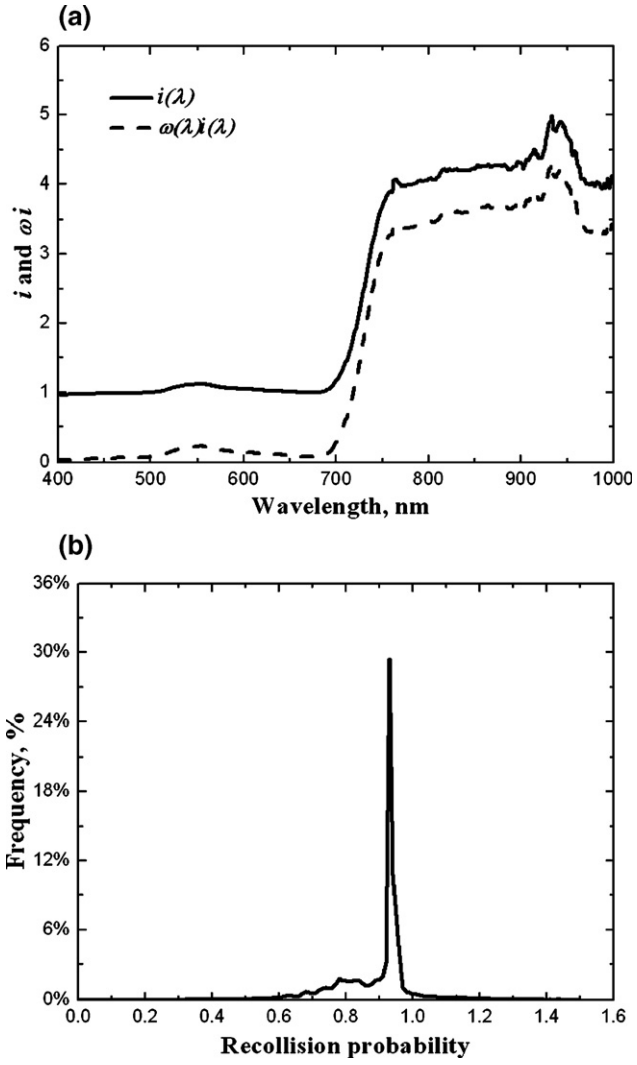

Fig. 2. Panel (a): mean number of photon–vegetation interactions (interaction coefficient), $i(\lambda)$ (solid line), and mean portion, $\omega(\lambda)i(\lambda)$ (dashed line), of scattered photons as a function of wavelength. Eqs. (2) and (3) are used to derive these curves from data shown in Fig. 1. Panel (b): frequency of values of the recollision probability calculated with Eq. (4) using all combinations of λ and λ_0 for which $\lambda > \lambda_0$ and $|\omega(\lambda)i(\lambda) - \omega(\lambda_0)i(\lambda_0)| > 0.001$. A negligible portion of the values exceeds unity due to ignoring the surface contribution (Wang et al., 2003) and measurement errors.

proportional to the difference, $\omega(\lambda)i(\lambda) - \omega(\lambda_0)i(\lambda_0)$, between portions of photons scattered by phytoelements at the same wavelengths, i.e., the ratio

$$p = \frac{i(\lambda) - i(\lambda_0)}{i(\lambda)\omega(\lambda) - i(\lambda_0)\omega(\lambda_0)}, \tag{4}$$

remains constant for any combinations of λ and λ_0 ($\lambda \neq \lambda_0$). The coefficient of proportionality, p, is the probability that a photon scattered from a phytoelement will interact within the canopy again—the recollision probability (Knyazikhin et al., 2005; Panferov et al., 2001; Smolander & Stenberg, 2005). Fig. 2b shows the frequency of values of the recollision probability corresponding to all combinations of λ and λ_0. Their distribution suggests that the ratio (4) is invariant with respect to the wavelength.

Setting $\omega(\lambda_0) = 0$, Eq. (4) can be rearranged to the form

$$i(\lambda)[1 - p\omega(\lambda)] = i_0. \tag{5}$$

This equation has a very simple interpretation. The probability that photons incident on phytoelements will be scattered and will interact within the canopy again is $p\omega(\lambda)$. The probability $1 - p\omega(\lambda)$, therefore, refers to those photons incident on phytoelements which either will be absorbed or will escape the vegetation as a result of the scattering event. The portion of intercepted photons, i_0, therefore, is the product of the mean number of photon-vegetation interactions, $i(\lambda)$, and the portion, $1 - p\omega(\lambda)$, of photons removed from the vegetation canopy as a result of one interaction.

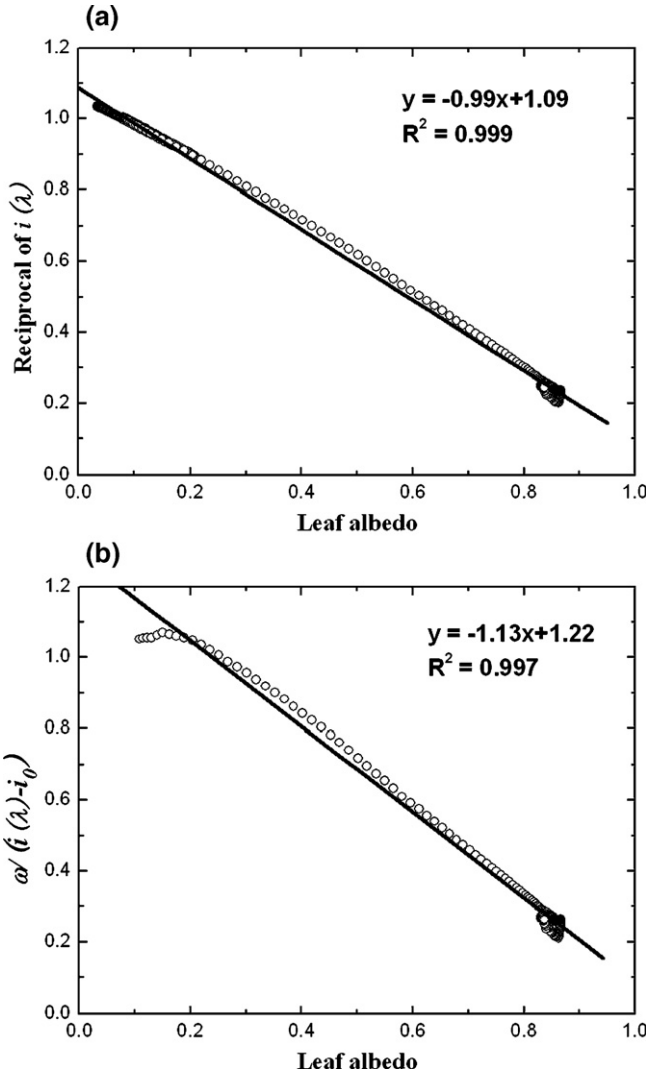

Fig. 3. (a) Reciprocal of $i(\lambda)$ and (b) $\omega(\lambda)/[i(\lambda) - i_0]$ versus values of the leaf albedo $\omega(\lambda)$ derived from data shown in Fig. 1. The recollision probability, $p = 0.91$, and canopy interceptance, $i_0 = 0.92$, are derived from the slope and intercept of the line in panel (a) first. The interceptance, $i_0 = 0.92$, is then used to calculate $\omega(\lambda)/[i(\lambda) - i_0]$. In order to avoid division by values close to zero, wavelengths for which $i(\lambda) - i_0 \geq 0.1$ are used to generate scatter plot in panel (b).

Eq. (5) can be rearranged to a different form which we use to derive p and i_0 from field data, namely,

$$\frac{1}{i(\lambda)} = \frac{1}{i_0} - \frac{p}{i_0}\omega(\lambda). \quad (6)$$

If the reciprocal of the canopy interaction coefficient calculated from measured canopy absorption and needle albedo (Eq. (3)) is plotted versus measured needle albedo, a linear relationship is obtained (Fig. 3a). The recollision probability, p, and canopy interceptance, i_0, can be specified from the slope and intercept.

Smolander and Stenberg (2005) suggested that the recollision probability may be assumed to remain constant in successive interactions. Given i_0, the interaction coefficient formulated for photons scattered one and more times is $j_1(\lambda)=i(\lambda)-i_0$. If the above assumption is true, then, as follows from Eq. (5), $j_1(\lambda)[1-p\omega(\lambda)]=p\omega(\lambda)i_0$, and thus, the ratio $\omega(\lambda)/j_1(\lambda)$ is a linear function with respect to the leaf albedo. As one can see from Fig. 3b, the data support the hypothesis of Smolander and Stenberg.

The canopy absorption coefficient, $a(\lambda)/i_0$, is the absorbed portion of photons from the incident beam that the canopy intercepts (Smolander & Stenberg, 2005). It follows from Eqs. (3) and (5) that

$$\frac{a(\lambda)}{i_0} = \frac{1-\omega(\lambda)}{1-p\omega(\lambda)}. \quad (7)$$

The portion of *intercepted* photons that escape the canopy in up- and downward directions, or canopy scattering coefficient, is $s(\lambda)/i_0=1-a(\lambda)/i_0$, i.e.,

$$\frac{s(\lambda)}{i_0} = \omega(\lambda)\frac{1-p}{1-p\omega(\lambda)}. \quad (8)$$

Fig. 4 shows correlation between canopy scattering coefficients derived from measured spectra (Fig. 1) using equation $1-a(\lambda)/i_0$ with $i_0=0.89$ (Fig. 3b) and from calculations using Eq. (8) with $p=0.93$ (Fig. 3b).

The canopy absorption and scattering coefficients link canopy spectral behavior at the *canopy* and the *leaf scales*. Indeed, the ratios $a(\lambda)/i_0$ and $s(\lambda)/i_0$ (*canopy scale*) are explicit functions of the leaf spectral albedo (*leaf scale*) and the wavelength-independent *recollision probability*. The recollision probability, therefore, is a scaling parameter that accounts for a cumulative effect of the canopy structure over a wide range of scales. Theoretical analyses (Knyazikhin et al., 1998) and Monte Carlo simulations (Smolander & Stenberg, 2005) suggest that the recollision probability is minimally sensitive to rather large changes in the direction of the incident beam. The canopy absorption and scattering coefficients, therefore, describe intrinsic canopy properties that determine the partitioning of the incident radiation into its absorbed and canopy leaving portions. One of the uses of these properties is in the interpretation of data acquired by spectroradiometers of different spectral bands and different resolutions (Disney et al., 2006; Knyazikhin et al., 1998; Myneni et al., 2002; Rautiainen & Stenberg, 2005; Tian et al., 2003; Wang et al., 2003).

2.2. Canopy spectral invariant for reflectance and transmittance

A scattered photon can escape the vegetation canopy through the upper or lower boundary with probabilities ρ and τ, respectively. Obviously, $\rho+\tau=1-p$. Unlike the recollision probability p (Fig. 3), the escape probabilities ρ and τ vary with the number of successive interactions. They, however, reach plateaus as the number of interactions increases (Lewis & Disney, 1998). The number of interaction events before this plateau is reached depends on the canopy structure and the needle transmittance–albedo ratio (Rochdi et al., 2006). Monte Carlo simulations of the radiation regime in 3D canopies suggest that the escape probabilities for up- and downward directions saturate after two to three photon–canopy interactions for low to moderate LAI canopies (Lewis & Disney, 1998). This result underlies the following approximation to the canopy reflectance proposed by Disney et al. (2005),

$$r(\lambda) = \omega(\lambda)R_1 + \frac{\omega(\lambda)^2 R_2}{1-p_r\omega(\lambda)}, \quad (9)$$

where R_1, R_2 and p_r are determined by fitting Eq. (9) to the measured reflectance spectrum.

If the probability ρ remains constant in successive interactions, then $R_1=\rho i_0$, $R_2=\rho p i_0$ and $p_r=p$. In this case, the first term gives the portion of photons from the incident flux that escape the vegetation canopy in upward directions as a result of one interaction with phytoelements. The second term accounts for photons that have undergone two and more interactions. Violation of the above condition results in a transformation of ρi_0, $\rho p i_0$ and p to some effective values R_1, R_2 and p_r as a result of the fitting procedure. The difference between the probabilities and their effective values depends on how fast the escape probability ρ reaches its plateau as the number of interactions increases. A detailed analysis of this effect will be given in

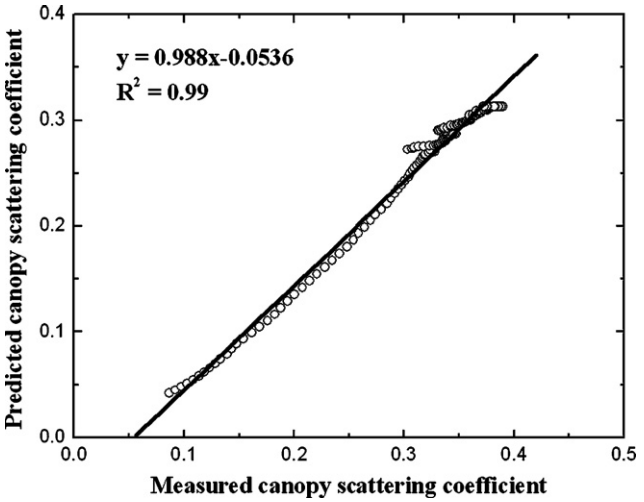

Fig. 4. Correlation between canopy scattering coefficients derived from data shown in Fig. 1 using equation $1-a(\lambda)/i_0$ and from calculations using Eq. (8). Data corresponding to the spectral interval $709\le\lambda\le900$ nm are used to generate this plot. This interval excludes the noisy data ($\lambda>900$ nm) and wavelengths for which $1-a(\lambda)/i_0<0.05$ ($\lambda\le709$ nm).

Sections 5 and 7. A simpler expression, assuming $R_2=p_rR_1$, can also be used, with a reduction in accuracy of the approximation (Disney and Lewis, 2005).

Fig. 5 shows correlation between measured canopy reflectance and canopy reflectance evaluated using Eq. (9) with $R_1=0.15$, $p_r=0.59$, and $R_2=p_rR_1=0.09$. One can see that field data follow the relationship predicted by Eq. (9) and therefore support the approximation proposed by Disney and Lewis. In this example, R_1 and p_r give the best fit to the measured reflectance spectrum. These coefficients can also be obtained from the slope and intercept of the regression line derived from values of the needle albedo ω and the reciprocal of r/ω at wavelengths from the interval between 700 nm and 750 nm. In this case, values of ω are uniformly distributed in the interval [0.1, 0.9] and the canopy reflectance exhibits a strong variation with ω. These features allow us to minimize the impact of ground reflection and measurement uncertainties on the specification of R_1 and p_r from the regression line.

Panferov et al. (2001) suggest that, if the needle transmittance to albedo ratio $\tau_L(\lambda)/\omega(\lambda)$ does not vary with the wavelength, the spectral invariant in the form of Eq. (5) holds in the relationship between canopy transmittance and leaf albedo, i.e.,

$$t(\lambda)=\frac{t_0}{1-p_t\omega(\lambda)}. \tag{10}$$

Here t_0 is the zero-order canopy transmittance defined as the probability that a photon in the incident radiation will arrive at canopy bottom without suffering a collision (Smolander & Stenberg, 2005). Analogous to Eq. (9), the use of the fitting procedure results in a transformation of the recollision probability to its effective value p_t due to neglecting variation in the escape probability τ with successive interactions. Fig. 6a shows correlation between measured canopy spectral transmittance (Fig. 1a) and canopy transmittance simulated with Eq. (10). Although Eq. (10) poorly approximates the observed canopy spectral transmittance in this particular case, the canopy interceptance, $i_0=0.92$ (Fig. 3a) and zero-order transmittance, $t_0=0.06$ (Fig. 6a), follow the expected relationship, $t_0+i_0=1$, sufficiently well. In this example, t_0 and p_t were specified by fitting Eq. (10) to the measured transmittance spectrum shown in Fig. 1a.

Fig. 6b shows correlation between measured canopy transmittance and canopy transmittance evaluated with an equation similar to Eq. (9), namely,

$$t(\lambda)=t_0+\frac{T_1\omega}{1-p_t\omega(\lambda)}, \tag{11}$$

where the coefficients t_0, T_1 and p_t are chosen by fitting Eq. (11) to the measured $t(\lambda)$. Analogous to Eq. (9), the coefficients T_1 and p_t are effective values of the probabilities τi_0, and p. It can be seen that a much better match with observed canopy spectral transmittances has been achieved. A theoretical analysis of this result will be given in Sections 5 and 7. It should be noted that canopy transmittance is sensitive to the needle transmittance–albedo ratio $\tau_L(\lambda)/\omega(\lambda)$ (Panferov et al., 2001; Rochdi et al., 2006). This may imbue wavelength dependence to the escape probabilities for low order scattered photons.

To summarize, field data on canopy and leaf transmittance and reflectance spectra support the validity of the theoretically derived spectral invariant relationships reported in literature. Two well-defined wavelength-independent variables, the recollision probability and canopy interceptance, and the wavelength-dependent leaf albedo determine the canopy absorptive properties at any wavelength of the solar spectrum. The non-absorbed portion of the incident radiation can be broken down into its reflected and transmitted portions. However, no clear physical interpretation of the canopy structure dependent coefficients, p_r and p_t, appeared in the spectral invariant relationships for canopy reflectance and transmittance has been reported. This currently hinders their use in remote sensing and model studies.

3. Canopy spectral invariants: mathematical basis

The data analysis presented in Section 2 suggests that the recollision and escape probabilities, their effective values and leaf optical properties allow for a simple parameterization of the spectral radiation budget of the vegetation canopy with non-reflecting background; that is, partitioning of the incoming radiation into canopy transmission, reflection and absorption at any wavelength in the solar spectrum. Its accuracy depends on how fast the escape probabilities reach their plateaus as the number of interactions increases. The aim of this section is to provide mathematical and physical bases for the process of photon–vegetation successive interactions. The formulations of Vladimirov (1963) and Marchuk et al. (1980) are adopted.

Let V and δV be the domain where radiative transfer occurs and its boundary, respectively. The domain V can be a shoot, tree crown, or a part of the vegetation canopy with several trees, etc. We use x and Ω to denote the spatial position and direction of the photon travel, respectively. We shall assume that (i) the domain V is bounded by a non-reflecting surface δV; (ii) the domain V is illuminated by a parallel beam; and (iii) the incident flux is unity (Appendix B.2). Let $Q_0(x,\Omega)$ be the distribution of

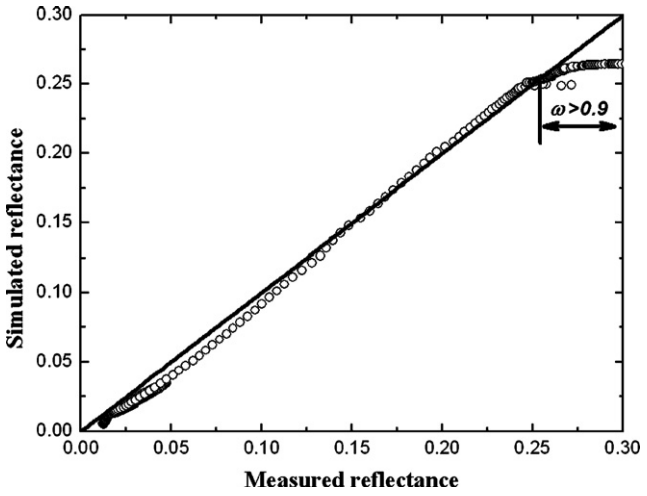

Fig. 5. Correlation between measured canopy reflectance and canopy reflectance evaluated using Eq. (9) with $R_1=0.15$, $p_r=0.59$, and $R_2=p_rR_1=0.09$ for the spectral interval $400\le\lambda\le900$ nm. The arrow indicates a range of reflectance values corresponding to $\omega\ge0.9$.

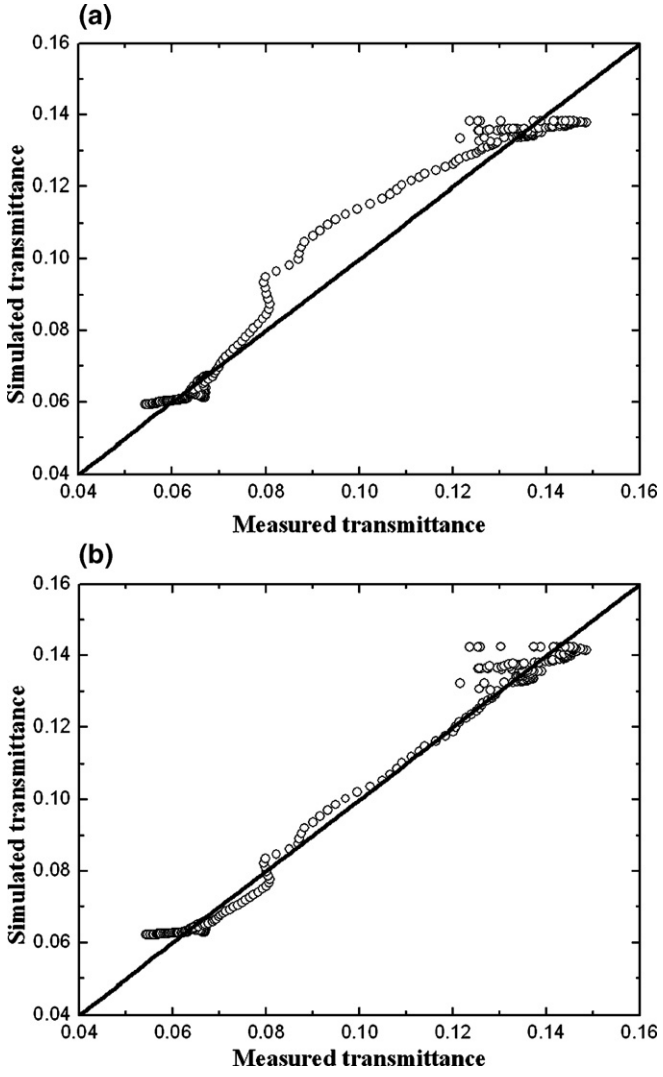

Fig. 6. Correlation between measured canopy transmittance and canopy transmittance simulated using (a) Eq. (10) with t_0=0.06, p_t=0.67 and (b) Eq. (11) with t_0=0.06, T_1=0.017 and p_t=0.94. In both cases, the sum of the canopy interceptance, i_0, (Fig. 3a) and t_0, is close to one, i.e., i_0+t_0=0.92+0.06=0.98.

uncollided photons in V defined as the probability density that a photon entering V will arrive at x along the direction Ω without suffering a collision. Under the conditions (i)–(iii), values of Q_0 do not depend on the wavelength.

Uncollided photons can either be absorbed or scattered as a result of the interaction with phytoelements. Given Q_0, the radiation field Q_1 generated by photons scattered once can be represented as $Q_1=TQ_0$. Here T is a linear operator that sets in correspondence to Q_0, the three-dimensional distribution of photons from Q_0 scattered by the vegetation canopy once. In the radiative transfer equation, it is an integral operator (Appendix B.5). In Monte Carlo models, T is a procedure that inputs Q_0, simulates the scattering event, calculates the photon free path and outputs the distribution, Q_1, of photons just before their next interaction with phytoelements. In terms of these notations, photons scattered m times can be expressed as $Q_m=TQ_{m-1}=T^mQ_0$. Unlike Q_0, the distribution Q_m depends on the wavelength λ. The distribution, $I_\lambda(x,\Omega)$, of photons in the domain V with a non-reflecting boundary δV can be expanded in successive order of scattering or, in Neumann series,

$$I_\lambda(x,\Omega) = Q_0 + TQ_0 + T^2Q_0 + \ldots + T^mQ_0 + \cdots \tag{12}$$

The following notations are introduced to investigate the Neumann series (12). Let $||f||$ be the interaction coefficient of a 3D radiation field $f(x,\Omega)$ in the domain V, i.e.,

$$||f|| = \int_{4\pi}\int_V \sigma(x,\Omega)|f(x,\Omega)|\mathrm{d}x\mathrm{d}\Omega, \tag{13}$$

where the integration is performed over the domain V and the unit sphere 4π. Here σ is the extinction coefficient; that is, $\sigma \mathrm{d}s$ is the probability that a photon while traveling a distance ds in the medium along the direction Ω will interact with the elements of the host medium. In terms of these notations, the canopy interaction coefficient, $i(\lambda)$, and canopy interceptance, i_0, are $||I_\lambda||$ and $||Q_0||$, respectively. The probability density, $e_m(x,\Omega)$, that a photon scattered m times will arrive at x along the direction Ω without suffering a collision can be expressed as

$$e_m(x,\Omega) = \frac{Q_m(x,\Omega)}{||Q_m||}. \tag{14}$$

A photon scattered m times will be scattered again with a probability of γ_{m+1} where

$$\gamma_{m+1} = \frac{||Q_{m+1}||}{||Q_m||}. \tag{15}$$

These probabilities are related as $Te_m=\gamma_{m+1}e_{m+1}$ (Appendix B.6). The recollision probability, p_{m+1} is therefore the ratio of γ_{m+1} to the single scattering albedo ω, i.e.,

$$p_{m+1} = \frac{\gamma_{m+1}}{\omega}. \tag{16}$$

The following mathematical results underlie the derivation of the spectral invariant relationships (Riesz & Sz.-Nagy, 1990; Vladimirov, 1963)

$$\lim_{m\to\infty}\gamma_m = \gamma_\infty, \qquad \lim_{m\to\infty} e_m(x,\Omega) = e_\infty(x,\Omega). \tag{17}$$

In general, the probabilities $e_m(x,\Omega)$ and γ_m vary with the scattering order m. However, they tend to reach plateaus as the number of interactions increases (Lewis & Disney, 1998). The limits γ_∞ and e_∞ are the unique positive eigenvalue of the operator T, corresponding to the unique positive (normalized to unity) eigenvector e_∞, i.e., $Te_m=\gamma_\infty e_\infty$ and $||e_\infty||=1$ (Vladimirov, 1963). These variables do not depend on the incident radiation (Appendix B.4).

The convergence process given by Eq. (17) means that γ_m and $e_m(x,\Omega)$ do not vary much with the order of scattering m if it exceeds a sufficiently large number, i.e., $\gamma_m \approx \gamma_\infty$, $e_m(x,\Omega)\approx e_\infty(x,\Omega)$ and $Te_m \approx \gamma_m e_m$ for m, $m+1$, $m+2$, …. The number m depends on the initial radiation field Q_0 which, in turn, is a function of the 3D canopy structure. Assuming negligible variation in γ_m and $e_m(x,\Omega)$ for the scattering order m and higher and

accounting for Eqs. (12) and (14), the radiation field $I_\lambda(x,\Omega)$ can be approximated as (Appendix B.6)

$$I_\lambda(x,\Omega) = I_{\lambda,m}(x,\Omega) + \delta_m, \tag{18}$$

where

$$I_{\lambda,m}(x,\Omega) = \sum_{k=0}^{m} ||Q_k||e_k + ||Q_m|| \frac{\gamma_{m+1}}{1-\gamma_{m+1}} e_{m+1}, \tag{19}$$

$$\delta_m = I_\lambda(x,\Omega) - I_{\lambda,m}(x,\Omega) \tag{20}$$

The radiation field $I_{\lambda,m}(x,\Omega)$ is the mth approximation to the 3D radiation field in the vegetation canopy, and δ_m is its error. Note that the non-negativity of e_k, $k=1,2,\ldots$, are critical to derive Eq. (20). Eqs. (18)–(20) underlie the derivation of the canopy spectral invariant relationships and their accuracies. It should be emphasized that these results are not tied to a particular canopy radiation model. The operator T represents any linear model that simulates the scattering event and the photon free path for photons from a given field. We will use the 3D radiative transfer equation to specify the operator T (Appendix B.5).

4. Canopy spectral invariant for the canopy interaction coefficient

Knyazikhin et al. (1998) showed that the spectral invariant relationship is accurate for $||I_\lambda e_\infty||$. The spectral invariant for the canopy interaction coefficient $i(\lambda)=||I_\lambda||$ is derived under the assumption that $||I_\lambda e_\infty|| \approx ||I_\lambda||$. The relationship given by Eq. (5), therefore is an approximation to $i(\lambda)$. Its accuracy depends on how fast the sequence $\gamma_m, m=1,2,\ldots$, converges to the eigenvalue γ_∞. The analysis of field data summarized in Fig. 3 suggests that variation in $p_m=\gamma_m/\omega$ with the scattering order is negligible, i.e., the "zero" approximation ($m=0$) provides an accurate estimate of $i(\lambda)$ and thus supports the above assumption. Here we examine the accuracy of the spectral invariant for the canopy interaction coefficient as a function of the scattering order m.

It follows form Eq. (19) that the mth approximation, $i_m(\lambda)$, to $i(\lambda)$ is

$$\begin{aligned} i_m(\lambda) &= \sum_{k=0}^{m} ||Q_k|| + ||Q_m|| \frac{\gamma_{m+1}}{1-\gamma_{m+1}} \\ &= i_0 \left(\sum_{k=0}^{m} \theta_k + \frac{\theta_{m+1}}{1-\gamma_{m+1}} \right). \end{aligned} \tag{21}$$

Here $i_0=||Q_0||$ is the canopy interceptance; $\theta_0=1$, and

$$\begin{aligned} \theta_k &= \frac{||Q_k||}{||Q_0||} = \frac{||Q_k||}{||Q_{k-1}||} \times \frac{||Q_{k-1}||}{||Q_{k-2}||} \times \cdots \times \frac{||Q_1||}{||Q_0||} \\ &= \gamma_1\gamma_2\cdots\gamma_k, k \geq 1. \end{aligned} \tag{22}$$

The error, δi_m, in the mth approximation can be estimated as (Appendix B.6)

$$|\delta i_m| = |i(\lambda) - i_m(\lambda)| \leq \varepsilon_{\gamma,m+1} \frac{\theta_{m+1}}{1-\gamma_{m+1}} s_{m+1} i_0, \tag{23}$$

where

$$\varepsilon_{\gamma,m+1} = \max_{k\geq 1} \frac{|\gamma_{m+1+k} - \gamma_{m+1}|}{\gamma_{m+1+k}}, \; s_{m+1} = \sum_{k=1}^{\infty} \frac{\theta_{m+1+k}}{\theta_{m+1}}. \tag{24}$$

Note that $\lim_{m\to\infty} \sqrt[m]{\theta_m} = \gamma_\infty$. If m is large enough, i.e., $\sqrt[m+1]{\theta_{m+1}} \approx \gamma_\infty$, the ratio $\theta_{m+1+k}/\theta_{m+1}$ can be approximated by γ_∞^k. Substituting this relationship into Eq. (24) one obtains $s_m \approx \gamma_\infty/(1-\gamma_\infty)$.

Two factors determine the accuracy of the mth approximation. The first one is the difference between successive approximations γ_{m+1} and γ_{m+1+k}; that is, the smaller this difference, the more accurate the approximation is. Examples shown in Fig. 3 suggest that the zero approximation provides an accurate spectral invariant relationship for the canopy interaction coefficient. Indeed, the canopy interceptances derived from two methods (Fig. 3)) and from the canopy spectral transmittance, $i_0=1-t_0$ (Fig. 6), agree well with each other. This can take place if $p_1 \approx p_2$.

The contribution of photons scattered $m+1$ or more times to the canopy radiation field is the second factor. Their contribution is given by $\theta_{m+1}/(1-\gamma_{m+1}) \approx \gamma_\infty^{m+1}/(1-\gamma_\infty)$ which depends on the recollision probability, p_∞, and the single scattering albedo, ω; that is, the higher $\gamma_\infty=p_\infty\omega$ is, the higher order of approximation is needed to estimate the canopy interaction coefficient. This is illustrated in Fig. 7. One can see that the difference p_2-p_1 reaches its maximum at high p values. The spectral invariant cannot be derived if $p_\infty\omega=1$ since the Neumann series (12) does not converge in this case.

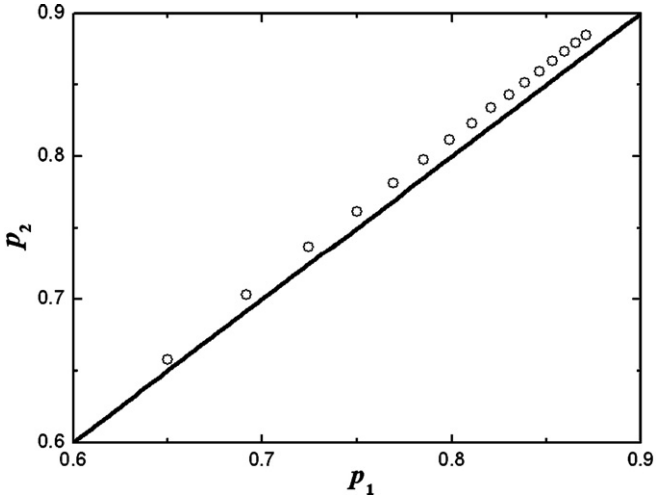

Fig. 7. Correlation between p_1 and p_2 for different values of leaf area index (LAI). Calculations were performed for a vegetation canopy consisting of identical cylindrical "trees" uniformly distributed in the canopy layer bounded from below by a non-reflecting surface. The canopy structure is parameterized in terms of the leaf area index of an individual tree, L_0, ground cover, g, and crown height, H. The LAI varies with the ground cover as LAI=gL_0. The stochastic radiative transfer equation (Appendix C) was used to derive canopy spectral interaction coefficient $i(\lambda)$ and canopy interceptance i_0 as a function of LAI. The first p_1, and second, p_2, approximations to the recollision probability were calculated as described in Section 2.1 using simulated values of $i(\lambda)$ and $i(\lambda)-i_0$. Here $\max\{|p_1-p_2|/p_1\}=0.02$. The crown height and plant LAI are set to 1 (in relative units) and 10, respectively. The solar zenith angle and azimuth of the incident beam are 30° and 0°.

5. Canopy spectral invariant for the canopy transmittance and reflectance

Let the domain V be a layer $0 \le z \le H$. The surfaces $z=0$ and $z=H$ constitute its upper and lower boundaries, respectively. We denote by $||f||_r$ and $||f||_t$ the upward flux at the canopy top and downward flux at the canopy bottom, respectively, of a radiation field $f(x,\Omega)$, i.e.,

$$||f||_r = \int_{z=0} \mathrm{d}r \int_{2\pi^+} \mathrm{d}\Omega f(r,\Omega)|\mu|,$$
$$||f||_t = \int_{z=H} \mathrm{d}r \int_{2\pi^-} \mathrm{d}\Omega f(r,\Omega)|\mu|, \quad (25)$$

where μ is the cosine of the zenith angle Ω and $2\pi^+$ ($2\pi^-$) denotes the upward (downward) hemisphere of directions. In terms of these notations, the canopy reflectance, $r(\lambda)$, and transmittance, $t(\lambda)$, are $||I_\lambda||_r$ and $||I_\lambda||_t$ (Appendix B.2).

Let ρ_m and τ_m be the probabilities that a photon scattered $m-1$ times will escape the vegetation canopy through the upper and lower boundary, respectively, as a result of interaction with a phytoelement (i.e., Appendix B.5)

$$\rho_m = \frac{1}{\omega}\frac{||T^m Q_0||_r}{||T^{m-1}Q_0||}, \quad \tau_m = \frac{1}{\omega}\frac{||T^m Q_0||_t}{||T^{m-1}Q_0||}. \quad (26)$$

$$\rho_m + \tau_m + p_m = 1. \quad (27)$$

We term ρ_m and τ_m escape probabilities. The escape probabilities vary with the scattering order. It follows from Eq. (17) that they reach plateaus as the number of interactions increases. We denote their limits by ρ_∞ and τ_∞.

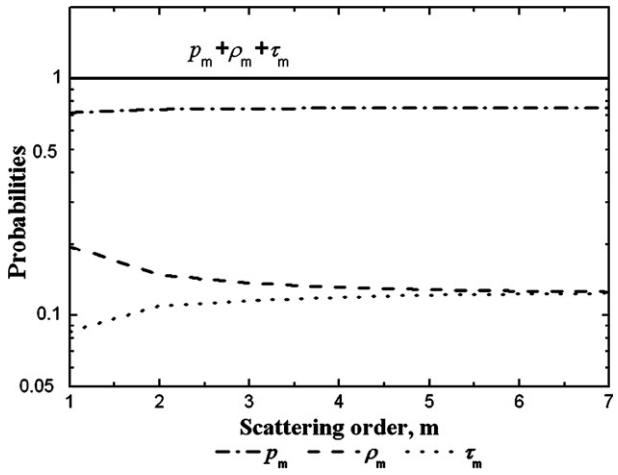

Fig. 8. Recollision probability, $p_m=\gamma_m/\omega$, and escape probabilities, τ_m and ρ_m, as a function of the scattering order m. Their limits are $p_\infty=0.75$, $\tau_\infty=0.125$ and $\rho_\infty=0.125$. The relative difference $\varepsilon_{\gamma,m+1}$ in the recollision probability is 3% for $m=0$ and 0.8% for $m=1$. The relative differences in escape probabilities are $\max_{k\ge1}|\tau_{3+k}-\tau_3|/\tau_{3+k} = 3.3\%$, and $\max_{k\ge1}|\rho_{3+k}-\rho_3|/\rho_{3+k} = 4\%$. Calculations were performed for the 3D vegetation canopy described in Fig. 7. Crown height, ground cover and plant LAI are set to 1, 0.16, and 10, respectively. The solar zenith angle and azimuth of the incident beam are 30° and 0°.

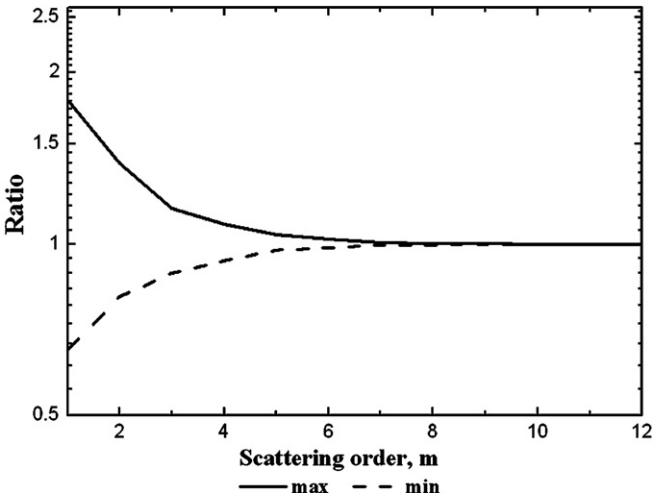

Fig. 9. Convergence of e_m to the positive eigenvector, e_∞, of the operator T. This plot shows variations in the ratios $\max_{\Omega\in2\pi^+}\{e_{m+1}/e_m\}$ (solid line) and $\min_{\Omega\in2\pi^+}\{e_{m+1}/e_m\}$ (dashed line) with the scattering order m. For $m\ge5$, their values fall in the interval between 0.98 and 1.04. Calculations were performed for the 3D vegetation canopy described in Fig. 7. Crown height, ground cover, plant, solar zenith angle and azimuth of the incident beam are the same as in Fig. 8.

It follows from Eq. (19) that the mth approximation, $r_m(\lambda)$ and $t_m(\lambda)$, to the canopy reflectance and transmittance are

$$r_m(\lambda) = ||I_{\lambda,m}||_r = \left[\sum_{k=1}^{m} \rho_k\theta_{k-1} + \frac{\theta_m\rho_{m+1}}{1-\gamma_{m+1}}\right]\omega i_0, \quad (28)$$

$$t_m(\lambda) = ||I_{\lambda,m}||_t = t_0 + \left[\sum_{k=1}^{m} \tau_k\theta_{k-1} + \frac{\theta_m\tau_{m+1}}{1-\gamma_{m+1}}\right]\omega i_0. \quad (29)$$

Here $t_0=1-i_0$ is the probability that that a photon in the incident radiation will arrive at canopy bottom without suffering a collision, i_0 is the canopy interceptance; and θ_k is defined by Eq. (22).

Errors in the mth approximation of canopy reflectance and transmittance can be estimated as (Appendix B.6)

$$|\delta r_m| = |r(\lambda)-r_m(\lambda)| \le \left(\varepsilon_{r,m+1}+\varepsilon_{\gamma,m+1}\right)\frac{\theta_m\rho_{m+1}}{1-\gamma_{m+1}}s_{r,m}\omega i_0, \quad (30)$$

$$|\delta t_m| = |t(\lambda)-t_m(\lambda)| \le \left(\varepsilon_{t,m+1}+\varepsilon_{\gamma,m+1}\right)\frac{\theta_m\tau_{m+1}}{1-\gamma_{m+1}}s_{t,m}\omega i_0. \quad (31)$$

Here is $\varepsilon_{\gamma,m}$ defined by Eq. (24) and

$$\varepsilon_{\kappa,m+1} = \max_{k\ge1}\frac{|\kappa_{m+1+k}-\kappa_{m+k}|}{\kappa_{m+k}}, \; s_{\kappa,m} = \sum_{k=1}^{\infty}\frac{\theta_{m+k}}{\theta_m}\frac{\kappa_{m+k}}{\kappa_{m+1}}, \quad (32)$$

where κ and κ_m represent either canopy reflectance ($\kappa=r$, $\kappa_m=\rho_m$) or canopy transmittance ($\kappa=t$, $\kappa_m=\tau_m$).

In addition to two factors that determine the accuracy in the mth approximation to the canopy interaction coefficient (cf.

Eq. (23)), δr_m and δt_m also depend on the proximity of two successive approximations κ_{m+k} and κ_{m+k+1} to the escape probabilities.

Thus, the errors in the mth approximations to the canopy reflectance and transmittance result from the errors in the recollision and escape probabilities, and from a contribution of multiple scattering photons to the canopy radiation regime. The mth approximation to the canopy reflectance and transmittance, therefore, is less accurate compared to the corresponding approximation to the canopy interaction coefficient. This is illustrated in Fig. 8. In this example, the relative difference $|\gamma_{m+1+k}-\gamma_{m+1}|/\gamma_{m+1+k}$ is 3% for $m=0$ and becomes negligible for $m\geq 1$. The zero and first approximations provide accurate spectral invariant relationships for the canopy interaction coefficient. The corresponding differences in the escape probabilities do not exceed 4% for $m\geq 2$, indicating that two scattering orders should be accounted to achieve an accuracy comparable to that in the zero approximation to the canopy interaction coefficient.

6. Canopy spectral invariant for bidirectional reflectance factor

The mth approximation, $I_{\lambda,m}(z=0,\Omega)$, to the canopy bidirectional reflectance factor (BRF), is given by Eq. (19). Its error, $|\delta_m(z=0,\Omega)|$ can be estimated as (Appendix B.6)

$$|\delta_m| \leq i_0 \frac{\theta_{m+1}}{1-\gamma_{m+1}} s_{BRF,m+1} \times \left[\max_{k\geq 1,\Omega\in 2\pi^+} \frac{|e_{m+1+k}(z=0,\Omega)-e_{m+k}(z=0,\Omega)|}{e_{m+k}(z=0,\Omega)} + \max_{k\geq 1} \frac{|\gamma_{m+k+1}-\gamma_{m+1}|}{\gamma_{m+k+1}} \right], \tag{33}$$

$$s_{\mathrm{BRF},m+1}(z=0,\Omega) = \sum_{k=1}^{\infty} \frac{\theta_{m+1+k}}{\theta_{m+1}} e_{m+k}(z=0,\Omega). \tag{34}$$

Here $2\pi^+$ in Eq. (33) denotes the upward hemisphere of directions. If m is large enough, i.e., $\sqrt[m+1]{\theta_{m+1}} \approx \gamma_\infty$ and $e_{m+1}\approx e_\infty$, the term $s_{\mathrm{BRF},m+1}$ can be approximated as $s_{\mathrm{BRF},m+1}\approx e_\infty\gamma_\infty/(1-\gamma_\infty)$. Its values, therefore, are mainly determined by the contribution of photons scattered $m+1$ and more times to the canopy radiation regime.

As it follows from Eq. (33), the accuracy in the mth approximation to the canopy BRF depends on the convergence of γ_{m+k} and e_{m+k} to the eigenvalue, γ_∞, and corresponding eigenvector, e_∞, of the operator T. Convergence of the former is illustrated in Fig. 8. Fig. 9 shows variations in $\max_{\Omega\in 2\pi^+}\{e_{m+1}/e_m\}$ and $\min_{\Omega\in 2\pi^+}\{e_{m+1}/e_m\}$ with the scattering order m. In this example, the difference $e_{m+1+k}-e_{m+k}$ is negligible for $m\geq 4$, indicating that the fourth approximation provides an accurate spectral invariant relationship for the canopy BRF. Variation in the probability e_m with the scattering order m should be accounted to evaluate the contribution of low-order scattered photons. Recently Rochdi et al. (2006) reported a sensitivity of the canopy BRF to the leaf transmittance, τ_L, versus albedo, ω, ratio. This result suggests that the number m at which e_m saturates is a function of τ_L/ω.

7. Zero-order approximations to the canopy spectral reflectance and transmittance

The theoretical analyses indicate that while the zero approximation is accurate for the canopy interaction coefficient, the canopy transmittance and reflectance require more iterations to achieve a comparable accuracy. The empirical analyses presented in Section 2 suggest that the zero approximations simulate observed spectral reflectance and transmittance sufficiently well if the recollision probability in the spectral invariant relationships is replaced with some effective values. Here we derive effective recollision probabilities for canopy reflectance and transmittance and examine accuracies in the modified zero approximations.

It follows from Eqs. (16), (22), (28) and (30) that the canopy spectral reflectance can be represented as

$$r(\lambda) = r_1(\lambda) + \delta r_1 = \left[\rho_1 + \frac{\omega p_1\rho_2}{1-p_2\omega} + \frac{\omega p_1\rho_2}{1-p_2\omega} S_{r,1}\right]\omega i_0 = \frac{1-\omega p_2 \Delta_{r,1}}{1-p_2\omega}\omega\rho_1 i_0. \tag{35}$$

Here $S_{r,1}$ is defined by Eq. (B10) and the term $\Delta_{r,1}$ characterizing the accuracy in the first approximation is

$$\Delta_{r,1} = 1-\frac{\rho_2}{\rho_1}\frac{p_1}{p_2}\left[1+S_{r,1}\right]. \tag{36}$$

The data analyses suggest that the reciprocal of the canopy spectral reflectance normalized by the leaf albedo ω varies "almost" linearly with ω (Section 2.2). Based on this observation, we replace the relationship between the reciprocal of $r/(\omega i_0\rho_1)$ and the leaf albedo ω with a regression line $Y=\alpha_r-\beta_r p_2\omega$. Coefficients R_1 and p_r in the approximation (9) with $R_2=p_rR_1$, can be specified from the slope β_r and intercept α_r, as

$$R_1 = \frac{i_0\rho_1}{\alpha_r}, \quad p_r = p_2\frac{\beta_r}{\alpha_r}, \tag{37}$$

$$\alpha_r = 1-2p_2\int_0^1 \frac{1-\Delta_{r,1}}{1-p_2\Delta_{r,1}\omega}\omega(2-3\omega)\mathrm{d}\omega, \quad \beta_r = 6\int_0^1 \frac{1-\Delta_{r,1}}{1-p_2\Delta_{r,1}\omega}\omega(2\omega-1)\mathrm{d}\omega. \tag{38}$$

Similarly, the canopy transmittance is

$$t(\lambda)-t_0 = \frac{T_1\omega}{1-p_t\omega}, \quad T_1 = \frac{i_0\tau_1}{\alpha_t}, \quad p_t = p_2\frac{\beta_t}{\alpha_t}. \tag{39}$$

Here α_t and β_t are given by Eq. (38) where $\Delta_{r,1}$ is calculated using the escape probabilities τ_1, τ_2, and the coefficient $S_{t,1}$ (see Eq. (B10) in Appendix B.6). We term this approach an 'inverse linear approximation'. Note that if the escape probabilities do not vary with the scattering order ($\Delta_{r,1}=\Delta_{t,1}=0$), the slopes and intercepts in the linear regressions models are equal to p_2 and unity, respectively, and the inverse linear approximation coincides with the zero approximation. If variations in the escape probabilities become negligible for $m\geq 2$, ($\varepsilon_{\kappa,2}\approx 0$, $\kappa=r,t$), the

effective probabilities p_r and p_t are functions of p_1, p_2, ρ_2, ρ_1 and p_1, p_2, τ_2, τ_1, respectively.

Fig. 10 shows variation in the reciprocal of $r(\lambda)/\omega$ and $(t(\lambda)-t_0)/\omega$ with the leaf albedo and the corresponding regression lines as well as recollision probability p_2 and its effective values, p_r and p_t, as functions of the leaf area index (LAI). Fig. 11 demonstrates the energy conservation relationships (27) for $m=1$. The escape probabilities are calculated from Eqs. (37) and (39) as R_1/i_0 and T_1/i_0. One can see that the impact of the regression coefficients α_r and α_t on the escape probabilities is minimal; that is, a deviation from the relationship $R_1/i_0+T_1/i_0+p_1=1$ does not exceed 5%. This is not surprising because values of $(1-\Delta_{\kappa,1})/(1-\Delta_{\kappa,1}p_2\omega)$ in Eq. (38) for α_r ($\kappa=r$) and α_t ($\kappa=t$) are multiplied by the function $\omega(2-3\omega)$ whose integral is zero. Note that the sum of the recollision and escape probabilities derived from field data is 1.06 (Figs. 3, 5 and 6b). A discrepancy of 6% is comparable to uncertainties due to the neglect of surface reflection (Fig. A1). The effective values of the recollision probabilities, p_r and p_t, however, depend on β_r and β_t (Fig. 10b).

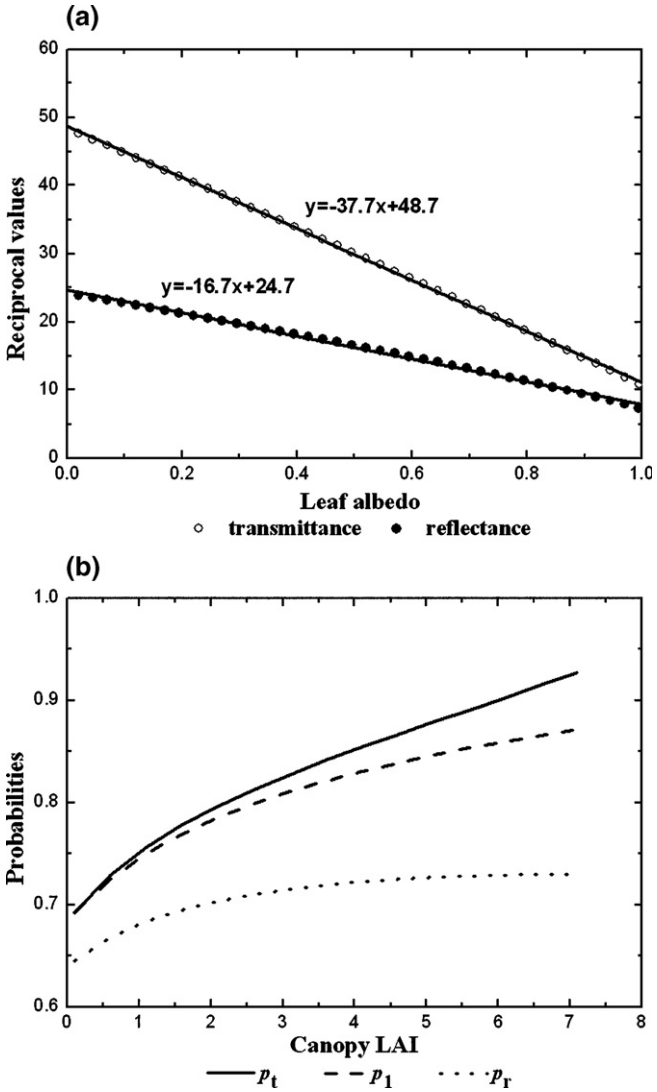

Fig. 10. (a) Reciprocal of $r(\lambda)/\omega$ and $(t(\lambda)-i_0)/\omega$ as functions of the leaf albedo and their linear regression models. (b) Recollision probability p_2 and its effective values p_r and p_t as functions of the LAI. Calculations are performed for the 3D vegetation canopy described in Fig. 7 with input parameters as in Fig. 8 (panel a) and Fig. 7 (panel b).

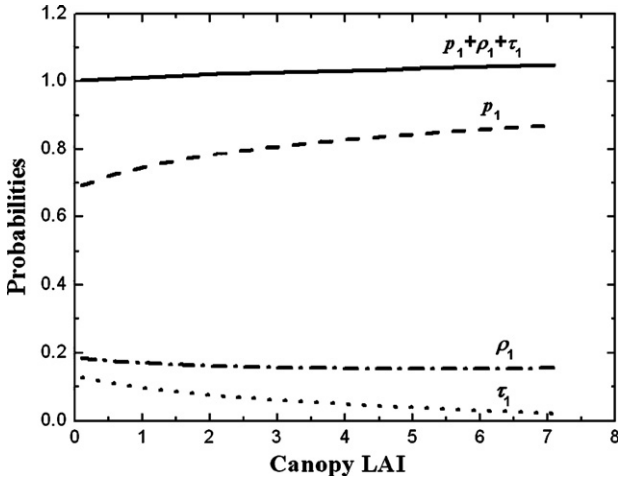

Fig. 11. Energy conservation relationship $\rho_1+\tau_1+p_1=1$ for different values of the leaf area index. The escape probabilities ρ_1 and τ_1 are calculated as the ratios of coefficients R_1 and T_1 in the inverse linear approximations to the canopy interceptance i_0, i.e., $\rho_1=R_1/i_0$ and $\tau_1=R_1/i_0$. The difference $\rho_1+\tau_1+p_1-1$ does not exceed +0.05. Calculations are performed for the 3D vegetation canopy described in Fig. 7. Note that the recollision and escape probabilities derived from field data (Figs. 3a and 6b) satisfy $\rho_1+\tau_1+p_1-1=0.06$.

Since eigenvalues and eigenvectors of the operator T are independent on the incident radiation, the limits p_∞, ρ_∞ and τ_∞ of the recollison and escape probabilities do not vary with the incident beam. Smolander and Stenberg (2005) showed that the first and higher orders of approximations to the recollision probability are insensitive to rather large changes in the solar zenith angle. Although the first approximations to the escape probabilities exhibit a higher sensitivity (Fig. 12) to the solar zenith angle, their sum, $\rho_1+\tau_1=1-p_1$, remains almost constant. This is consistent with our theoretical results suggesting that the

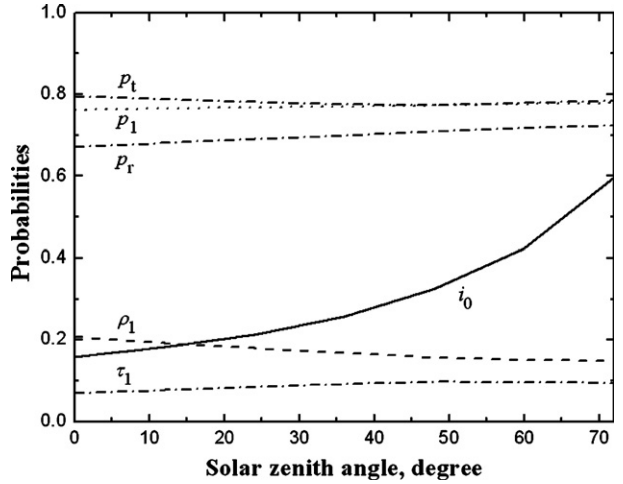

Fig. 12. Recolision probability, p_1, its effective values, p_r and p_t, escape probabilities, ρ_1 and τ_1, and the canopy interceptance, i_0, as functions of the solar zenith angle. Eq. (26) is used to specify ρ_1 and τ_1. Calculations are performed for the 3D vegetation canopy described in Fig. 7 with input parameters as in Fig. 8.

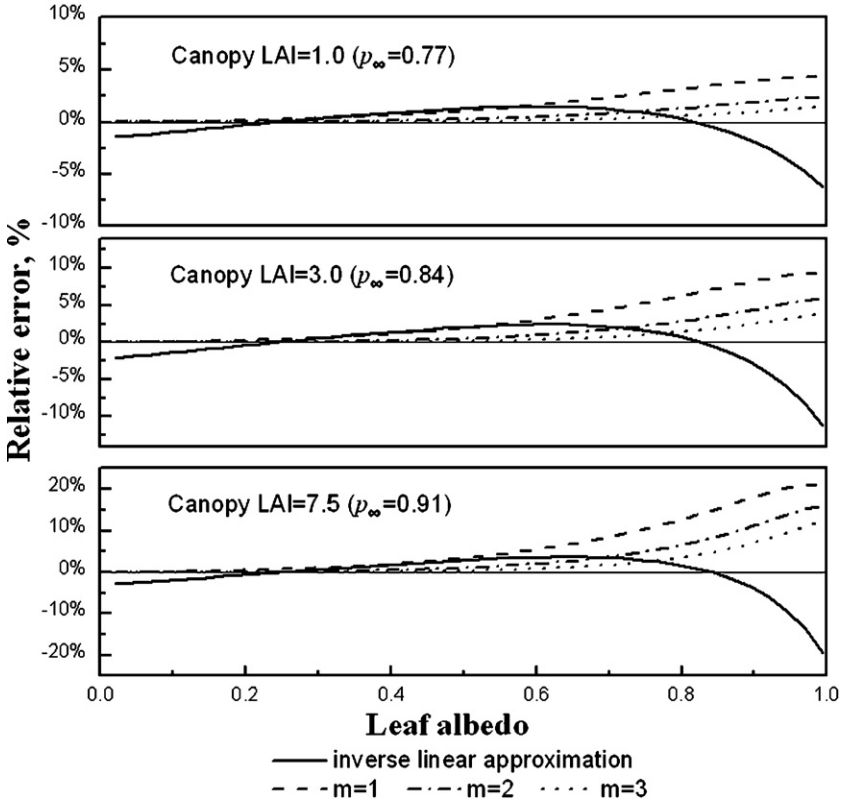

Fig. 13. Relative error in the canopy reflectance as a function of the single scattering albedo for three values of canopy leaf area index, 1, 3 and 7.5.

canopy interaction coefficient requires less iterations to reach a plateau compared to the canopy reflectance and transmittance. The sensitivity of the effective recollision probabilities to the solar zenith angle is much smaller compared to the canopy interceptance.

Fig. 13 shows relative errors in the inverse linear approximation and the mth approximations, $m=1$, 2 and 3, to the canopy reflectance as a function of the leaf albedo and leaf area index. The error decreases with the scattering order. For a fixed m, it increases with the leaf albedo and canopy leaf area index. This is consistent with the theoretical results stating that the convergence depends on the maximum eigenvalue $\gamma_\infty = p_\infty \omega$; that is, the higher its value is, the higher order of approximation is needed to estimate the canopy reflectance. In this example, the third and inverse linear approximations have the same accuracy level, i.e., they are accurate to within 5% if $\omega \leq 0.9$. The data analyses do not reject this conclusion (Fig. 5). The relative error in the canopy transmittance (not shown here) exhibits similar behavior. More advanced approaches that provide the best fit not only to the canopy reflectance and transmittance but also to the shortwave energy conservation law are discussed in Disney et al. (2005).

8. Conclusions

Empirical analyses of spectral canopy transmittance and reflectance collected during a field campaign in Flakaliden, Sweden, June 25–July 4, 2002, support the validity of the theoretically derived spectral invariant relationships reported in literature; that is, a small set of well-defined measurable wavelength-independent parameters specify an accurate relationship between the spectral response of a vegetation canopy with non-reflecting background to incident solar radiation at the leaf and the canopy scale. This set includes the recollision and escape probabilities, the canopy interceptance and the effective recollision probabilities for canopy reflectance and transmittance. In terms of these variables, the partitioning of the incident solar radiation between canopy absorption, transmission and reflection can be described by explicit expressions that relate leaf spectral albedo to canopy absorptance, transmittance and reflectance spectra.

In general case, the recollision and escape probabilities vary with the scattering order. The probabilities, however, reach plateaus as the number of interactions increases. The canopy spectral invariant relationships are valid for photons scattered m and more times where m is the number of scattering events at which the plateaus are reached. Contributions of these photons to canopy absorption, transmission and reflection can be accurately approximated by explicit functions of saturated values of the recollision and escape probabilities, the single scattering albedo and the canopy interceptance. Variation in the probabilities with the scattering order should be accounted to evaluate the contribution of low order scattered photons.

The numerical and empirical analyses suggest that the recollision probability reaches its plateau after the first scattering event. This is a sufficient condition to obtain the spectral

invariant for the canopy interaction coefficient that accounts for all scattered photons. The theoretical and numerical analysis indicates the escape probabilities require at least one more scattering event to reach the plateau. The theoretical, numerical and data analyses, however, suggest that the spectral invariant for canopy reflectance and transmittance can be applied to all scattered photons if one replaces the recollision probability in the spectral invariant relationships for canopy reflectance and transmittance with the some effective values. Their accuracies depend on the product of the recollision probability and single scattering albedo; that is, the higher these values are, the lower their accuracies. The numerical analysis suggests that the relative errors in the spectral invariant relationships for canopy transmittance and reflectance do not exceed 5% as long as the single scattering albedo is below 0.9. The recollision probability, its effective values and escape probabilities are appeared to be minimally sensitive to rather large changes in the solar zenith angle.

The probability density that a photon scattered m times will escape the vegetation canopy in a given upward direction converges to the wavelength-independent positive eigenvector of the transport equation as the number m of interactions increases. This property allows us to formulate the spectral invariant for the canopy bidirectional reflectance factor; that is, the angular signature of photons scattered m and more times is proportional to the positive eigenvector. The coefficient of proportionality is an explicit function of the single scattering albedo, the recollision probability and the number m of scattering events. The numerical analysis suggests that the convergence can be achieved after three to four interactions.

Recall that the spectral invariant relationships are valid for vegetation canopy bounded from below by a non-reflecting surface. The three-dimensional radiative transfer problem with arbitrary boundary conditions can be expressed as a superposition of the solutions of some basic radiative transfer subproblems with purely absorbing boundaries to which the spectral invariant is applicable (Davis & Knyazikhin, 2005; Knyazikhin & Marshak, 2000; Knyazikhin et al., 2005; Wang et al., 2003). This property and the results of this paper suggest that spectral response of the vegetation canopy to the incident solar radiation can be fully described by a small set of independent variables which includes spectra of surface reflectance and leaf albedo, the wavelength-independent canopy interceptance, recollision probability, its effective values and escape probabilities. This has significant implications for the effective exploitation of canopy radiation measurements and modelling methods. In particular, it allows for the decoupling of the structural and radiometric components of the scattered signal. This in turn permits better quantification and understanding of the structural and biochemical (wavelength-dependent) components of the signal, which by necessity are generally considered in a coupled sense.

Acknowledgment

This research was funded by the NASA EOS MODIS and MISR projects under Contracts NNG04HZ09C and 1259071, by the NASA Earth Science Enterprise under Grant G35C14G2 to Georgia Institute of Technology. M. Rautiainen and P. Stenberg were supported by Helsinki University Research Funds. M. Disney and P. Lewis received partial support through the NERC Centre for Terrestrial Carbon Dynamics. We also thank the anonymous reviewer for her/his comments, which led to a substantial improvement of the paper.

Appendix A. Field data

A.1. Description of field campaign and measurements

The Flakaliden field campaign was conducted between June 25 and July 4, 2002 with the objective of collecting data needed for validation of satellite derived leaf area index (LAI) and fraction of photosynthetically active radiation (FPAR) absorbed by the vegetation canopy. There were 39 participants from seven countries: Sweden, Finland, United States, Italy, Germany, Estonia, and Iceland. Flakaliden is located in northern Sweden, a region dominated by boreal forests. Canopy spectral transmittance and reflectance, soil and understorey reflectance spectra, needle optical properties, shoot structure and LAI were collected in six 50 m × 50 m plots composed of Norway spruce (*Picea abies* (L.) Karst) located at Flakaliden Research Area (64°14′N, 19°46′E) operated by the Swedish University of Agricultural Sciences. Each plot has its own variables and controls to determine factors that influence tree growth, i.e., experimental treatments of the plots involve tree response to variations in irrigation and fertilization. Data collected in an irrigated and fertilized plot (plot 9A) are used in Section 2.

Simultaneous measurements of spectral up- and downward radiation fluxes below, and upward radiation fluxes above the 50 m × 50 m plots from 400 nm to 1000 nm at 1.6 nm spectral resolution were obtained with two ASD hand-held spectroradiometers (Analytical Spectral Devices Inc., 1999). A helicopter was used to take ASD measurements above the center of each plot at heights of 15, 30 (used in this study), and 45 m. The ASD field of view was set to 25°. A LICOR LI-1800 spectroradiometer (LI-COR, 1989) with standard cosine receptor was placed in an open area to record spectral variation of incident radiation flux density between 300–1100 nm at 1 nm spectral resolution. All spectroradiometers were inter-calibrated by taking a series of simultaneous measurements of downward fluxes in an open area. We followed the methodology of Wang et al. (2003) to convert the measured spectra to canopy spectral reflectance and transmittance. Note that the spectral measurements were made under ambient atmospheric conditions of direct and diffuse illumination. This can cause some "spikes" in spectral downward radiation fluxes at the Earth's surface (Fig. 1a), e.g., due to variation in the fraction of the direct radiation (Verhoef, 2004). The impact of direct and diffuse components of the incident radiation on canopy spectral invariant relationships is discussed in Wang et al. (2003).

Current year, 1-year and 2-year-old spruce needles were sampled from six different heights in the control and irrigated with complete fertilizer plots and their transmittances and reflectance spectra were measured under laboratory conditions

using ASD FieldSpec Pro spectroradiometer and LICOR LI-1800-12s External Integrating Sphere (LI-COR, 1989). We followed the measurement methodology documented in (Daughtry et al., 1989; Mesarch et al., 1999). Needle spectral reflectance and transmittance of an average needle were obtained by averaging 50 measured spectra with a high weight given to the 2-year-old needles (80%) and equal weights to the current (10%) and 1-year (10%) needles. More details about instrumentation and measurement approach can be found in WWW1 (2002).

A.2. Uncertainties due to the neglect of surface reflection

In the framework on one-dimensional radiative transfer equation, the canopy transmittance, $t(\lambda)$, reflectance, $r(\lambda)$, and absorptance, $a(\lambda)$, can be represented as (Knyazikhin & Marshak, 2000; Wang et al., 2003)

$$t(\lambda) = \frac{t_{\mathrm{BS}}(\lambda)}{1-\rho_{\mathrm{sur}}(\lambda)r_{\mathrm{S}}(\lambda)} = t_{\mathrm{BS}}(\lambda) + t(\lambda)\rho_{\mathrm{sur}}(\lambda)r_{\mathrm{S}}(\lambda), \quad \text{(A1)}$$

$$r(\lambda) = r_{\mathrm{BS}}(\lambda) + t(\lambda)\rho_{\mathrm{sur}}(\lambda)t_{\mathrm{S}}(\lambda), \quad \text{(A2)}$$

$$a(\lambda) = a_{\mathrm{BS}}(\lambda) + t(\lambda)\rho_{\mathrm{sur}}(\lambda)a_{\mathrm{S}}(\lambda). \quad \text{(A3)}$$

Here, ρ_{sur} is the hemispherical reflectance of the canopy ground. Variables r_{BS} and r_{S}; t_{BS} and t_{S}; a_{BS} and a_{S} denote canopy reflectance, transmittance, and absorptance calculated for a vegetation canopy (1) illuminated from above by the incident radiation and bounded from below by a non-reflecting surface (subscript "BS", for black soil); and (2) illuminated from the bottom by normalized isotropic sources and bounded from above by a non-reflecting boundary (subscript "S"). These variables are related via the energy conservation law, i.e., $a_i+r_i+t_i=1$, i=BS, S.

The canopy spectral invariants are formulated for t_{BS}, r_{BS} and a_{BS}. In Section 2, the measured spectral transmittance, t, and reflectance, r, are taken as estimates of r_{BS} and t_{BS}. The absorptance a_{BS} is approximated using Eq. (1). It follows from Eqs. (A1)–(A3) that the relative errors, Δ_a, Δ_t and Δ_r, and in a_{BS}, t_{BS} and r_{BS} due to the neglect of surface reflection can be estimated in terms of t, r and ρ_{sur} measured during the Flakaliden field campaign as

$$\Delta_a = \frac{a_{\mathrm{BS}}-(1-r-t)}{1-t-r} = \frac{t}{1-t-r}\rho_{\mathrm{sur}}(t_{\mathrm{S}}+r_{\mathrm{S}}) \le \frac{t}{1-t-r}\rho_{\mathrm{sur}}, \quad \text{(A4)}$$

$$\Delta_t = \frac{t-t_{\mathrm{BS}}}{t} = \rho_{\mathrm{sur}}r_{\mathrm{S}} \le \rho_{\mathrm{sur}},\ \Delta_r = \frac{r-r_{\mathrm{BS}}}{r} = \frac{t}{r}\rho_{\mathrm{sur}}t_s \le \frac{t}{r}\rho_{\mathrm{sur}}, \quad \text{(A5)}$$

Thus, our approximations overestimate t_{BS} and r_{BS}, and underestimate a_{BS}. Since neglected terms t_{S}, r_{S}, and $t_{\mathrm{S}}+r_{\mathrm{S}}$ are below unity, Eqs. (A4) and (A5) provide the upper limits of Δ_a, Δ_t, and Δ_r. Fig. A1 shows upper limits of the relative errors as a function of the wavelength. As one can see, measured canopy absorptance approximates a_{BS} with an accuracy of about 5%. Deviations of measured canopy transmittance and reflectance from t_{BS} and r_{BS} in the interval $400 \le \lambda \le 700$ nm do not exceed 5%. Contribution of the canopy ground to transmittance and reflectance in the interval $700 \le \lambda \le 900$ nm is significant and cannot be ignored.

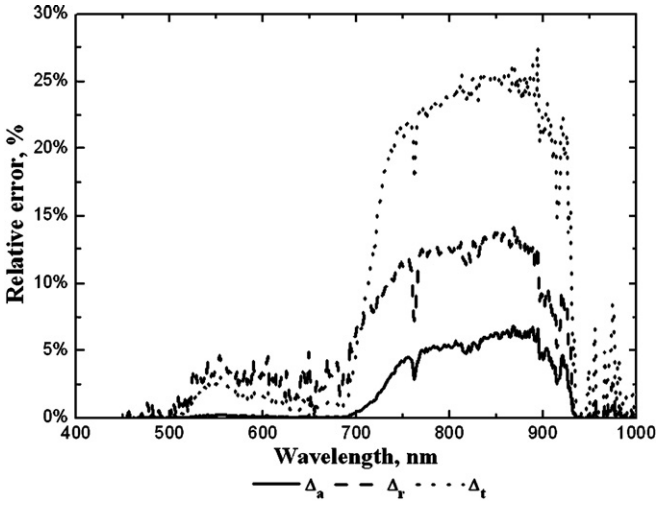

Fig. A1. Upper limits of the relative errors Δ_t, Δ_r, and Δ_a in estimates of t_{BS}, r_{BS} and a_{BS} due to the neglect of surface reflection.

Appendix B. 3D radiative transfer equation and its properties

Below, the formulation of the radiative transfer in three-dimensional vegetation canopies of Knyazikhin et al. (2005) is adopted. The mathematical theory of the radiative transfer equation can be found in Vladimirov (1963).

B.1. Operator notations

Let L and S_λ be the streaming-collision and scattering linear operators defined as

$$\begin{aligned} LJ_\lambda &= \Omega \bullet \nabla J_\lambda(x,\Omega) + \sigma(x,\Omega)J_\lambda(x,\Omega), \\ S_\lambda J_\lambda &= \int_{4\pi} \sigma_{s,\lambda}(x,\Omega' \to \Omega)J_\lambda(x,\Omega')\mathrm{d}\Omega'. \end{aligned} \quad \text{(B1)}$$

Here $\Omega \bullet \nabla J_\lambda$ is the directional derivative that quantifies change in $J_\lambda(x,\Omega)$ near x in direction Ω; σ and $\sigma_{s,\lambda}$ are the total interaction cross-section (extinction coefficient) and differential scattering coefficient. These coefficient are related as

$$\int_{4\pi} \sigma_{s,\lambda}(x,\Omega' \to \Omega)\mathrm{d}\Omega = \omega(x,\Omega')\sigma(x,\Omega'), \quad \text{(B2)}$$

where ω is the single scattering albedo (Knyazikhin et al., 2005). For ease of analysis, we assume that the single scattering albedo does not depend on x and Ω'. It coincides with the leaf albedo in this case. In radiative transfer in vegetation canopies,

the extinction coefficient does not depend on the wavelength (Ross, 1981).

B.2. Boundary conditions

Let the domain V be illuminated by a parallel beam of unit intensity. Interaction of shortwave radiation with the vegetation canopy in V is described by the following boundary value problem for the 3D radiative transfer equation (Knyazikhin et al., 2005; Ross, 1981)

$$LJ_\lambda = S_\lambda J_\lambda, \tag{B3}$$

$$J_\lambda(x_b, \Omega) = \delta(\Omega - \Omega_0), \quad x_b \in \delta V, \quad \Omega \bullet n_b < 0. \tag{B4}$$

Here Ω_0 is the direction of the incident beam; n_b is the outward normal at point $x_b \in \delta V$, and $J_\lambda(x,\Omega)$ is the monochromatic intensity which depends on the wavelength, λ, location x and direction Ω. The flux, $F^\downarrow$, of radiation incident on the canopy boundary is given by $F^\downarrow = \int_{\delta V} |n_b \bullet \Omega_0| \mathcal{H}(-n_b \bullet \Omega_0) dr_b$ where $\mathcal{H}$ is the Heaviside function. For boundary conditions used in Section 5, $F^\downarrow = |\mu_0| \delta V_t$ where μ_0 is the cosine of the polar angle of Ω_0 and δV_t is the area of the canopy upper boundary. The boundary condition for the lower boundary is set to zero. Under conditions (i)–(iii) (see Section 3), the intensity, $I_\lambda(x,\Omega)$, of radiation field in V is given by the solution of the boundary value problem (B3) and (B4) normalized by $F^\downarrow$, i.e., $I_\lambda = J_\lambda / F^\downarrow$.

B.3. Comments on Eq. (17)

In the framework of functional analysis, Eq. (13) is a norm in the Banach space of integrable functions, and T is a linear operator acting in this space. Eq. (17) are valid for any linear operator satisfying some general conditions (Riesz & Sz.-Nagy, 1990) which are met for the three-dimensional transport equation (Vladimirov, 1963) and Monte Carlo models of the radiative transfer (Marchuk et al., 1980).

B.4. Eigenvectors and eigenvalues of the radiative transfer equation

An eigenvalue of the radiative transfer equation is a number γ such that there exists a function $e(x,\Omega)$ that satisfies $\gamma Le = S_\lambda e$ and zero boundary conditions. Since the eigenvalue and eigenvector problem is formulated for zero boundary conditions, γ and $e(x,\Omega)$ are independent on the incoming radiation. Under some general conditions (Vladimirov, 1963), the set of eigenvalues and eigenvectors is a discrete set. The radiative transfer equation has a unique positive eigenvalue, γ_∞, that corresponds to a unique positive eigenvector, e_∞ (Vladimirov, 1963).

B.5. Successive orders of scattering approximations

The intensity, $I_\lambda(x,\Omega)$, satisfies the integral radiative transfer equation $I_\lambda = TI_\lambda + Q_0$ (Knyazikhin et al., 2005). Here $T = L^{-1} S_\lambda$, and Q_0 satisfies $LQ_0 = 0$ and the boundary conditions (B4) normalized by the incident flux $F^\downarrow$. The boundary conditions and the streaming-collision operator do not depend on wavelength, and thus, Q_0 is wavelength independent. The solution $I_\lambda = (E-T)^{-1} Q_0$ to the integral radiative transfer equation can be expanded in the Neumann series (12) where $Q_m = T^m Q_0$ satisfies the equation $LQ_m = S_\lambda Q_{m-1}$ and zero boundary conditions. The symbol E denotes the identity operator. Integrating this equation over spatial and directional variables and taking into account Eq. (B2), one obtains the following energy conservation relationships

$$||T^m Q_0||_r + ||T^m Q_0||_t + ||T^m Q_0|| = \omega ||T^{m-1} Q_0||. \tag{B5}$$

Eq. (27) is obtained by dividing Eq. (B5) by $\omega ||T^{m-1} Q_0||$.

It follows from Eqs. (26) and (14) that

$$\begin{aligned} \rho_m &= \frac{1}{\omega} \frac{||T^m Q_0||_r}{||T^{m-1} Q_0||} = \frac{1}{\omega} \frac{||T^m Q_0||}{||T^{m-1} Q_0||} \frac{||T^m Q_0||_r}{||T^m Q_0||} \\ &= \frac{\gamma_m}{\omega} ||e_m||_r. \end{aligned} \tag{B6}$$

This equation can be rewritten as $||e_m||_r = \omega \rho_m / \gamma_m$. Similarly, $||e_m||_t = \omega \tau_m / \gamma_m$.

B.6. Error in the mth approximation

It follows from Eq. (14) that

$$\gamma_{m+1} e_{m+1} = \frac{||Q_{m+1}||}{||Q_m||} \frac{Q_{m+1}}{||Q_{m+1}||} = \frac{TQ_m}{||Q_m||} = Te_m. \tag{B7}$$

Taking into account the operator identity $\sum_{k=0}^{\infty} T^k = (E-T)^{-1}$ and Eq. (B7), one gets

$$\begin{aligned} \delta_m &= I_\lambda(x,\Omega) - I_{\lambda,m}(x,\Omega) \\ &= T\left(\sum_{k=0}^{\infty} T^k\right) T^m Q_0 - ||Q_m|| \frac{\gamma_{m+1}}{1-\gamma_{m+1}} e_{m+1} \\ &= ||Q_m|| \left[T\left(E-T\right)^{-1} e_m - \frac{1}{1-\gamma_{m+1}} Te_m \right] \\ &= ||Q_m|| T\left(E-T\right)^{-1} \left[e_m - \frac{1}{1-\gamma_{m+1}} (E-T) e_m \right] \\ &= ||Q_m|| T\left(E-T\right)^{-1} \left[e_m - \frac{1}{1-\gamma_{m+1}} e_m + \frac{\gamma_{m+1} e_{m+1}}{1-\gamma_{m+1}} \right] \\ &= ||Q_m|| \frac{\gamma_{m+1}}{1-\gamma_{m+1}} \sum_{k=1}^{\infty} \left(T^k e_{m+1} - T^k e_m \right). \end{aligned}$$

It follows from Eqs. (B7) and (22) that

$$\begin{aligned} \delta_m &= i_0 \frac{\theta_{m+1}}{1-\gamma_{m+1}} \sum_{k=1}^{\infty} \frac{\theta_{m+k+1}}{\theta_{m+1}} \left(e_{m+k+1} - \frac{\gamma_{m+1}}{\gamma_{m+1+k}} e_{m+k} \right) \\ &= i_0 \frac{\theta_{m+1}}{1-\gamma_{m+1}} \sum_{k=1}^{\infty} \frac{\theta_{m+k+1}}{\theta_{m+1}} \left(e_{m+k+1} - e_{m+k} + \frac{\gamma_{m+1+k} - \gamma_{m+1}}{\gamma_{m+1+k}} e_{m+k} \right). \end{aligned} \tag{B8}$$

The upper bound to the error δ_m follows directly from Eq. (B8).

Let κ and κ_m represent either canopy reflectance ($\kappa=r$, $\kappa_m=\rho_m$) or canopy transmittance ($\kappa=t$, $\kappa_m=\tau_m$). Integrating $\delta_m|\mu|$ over the upward (downward) directions and taking into account Eqs. (22), (26) and (B6) one gets

$$\begin{aligned}\delta\kappa_m &= ||\delta_m||_\kappa \\ &= i_0\frac{\theta_{m+1}}{1-\gamma_{m+1}}\sum_{k=1}^{\infty}\frac{\theta_{m+k+1}}{\theta_{m+1}}\left(||e_{m+k+1}||_\kappa-\frac{\gamma_{m+1}}{\gamma_{m+1+k}}||e_{m+k}||_\kappa\right)\\ &= i_0\frac{\theta_m}{1-\gamma_{m+1}}\sum_{k=1}^{\infty}\frac{\theta_{m+k+1}}{\theta_m}\left(\frac{\omega\kappa_{m+1+k}}{\gamma_{m+1+k}}-\frac{\gamma_{m+1}}{\gamma_{m+1+k}}\frac{\omega\kappa_{m+k}}{\gamma_{m+k}}\right)\\ &= \omega i_0\frac{\theta_m}{1-\gamma_{m+1}}\sum_{k=1}^{\infty}\frac{\theta_{m+k}}{\theta_m}\left(\kappa_{m+1+k}-\frac{\gamma_{m+1}}{\gamma_{m+k}}\kappa_{m+k}\right)\\ &= \omega i_0\frac{\theta_m\kappa_{m+1}}{1-\gamma_{m+1}}\sum_{k=1}^{\infty}\frac{\theta_{m+k}}{\theta_m}\frac{\kappa_{m+k}}{\kappa_{m+1}}\left(\frac{\kappa_{m+1+k}}{\kappa_{m+k}}-\frac{\gamma_{m+1}}{\gamma_{m+k}}\right)\\ &= \omega i_0\frac{\theta_m\kappa_{m+1}}{1-\gamma_{m+1}}S_{\kappa,m},\end{aligned} \tag{B9}$$

where

$$S_{\kappa,m}=\sum_{k=1}^{\infty}\frac{\theta_{m+k}}{\theta_m}\frac{\kappa_{m+k}}{\kappa_{m+1}}\left(\frac{\kappa_{m+1+k}-\kappa_{m+k}}{\kappa_{m+k}}+\frac{\gamma_{m+k}-\gamma_{m+1}}{\gamma_{m+k}}\right). \tag{B10}$$

It follows from Eq. (B10) that $|S_{\kappa,m}|\le(\varepsilon_{\kappa,m+1}+\varepsilon_{\gamma,m+1})s_{\kappa,m}$. Estimate (23) can be obtained in a similar manner.

Appendix C. Simulation of the 3D canopy radiation regime

The domain V is a parallelepiped of horizontal dimensions X_d, Y_d, and height H. The top, δV_t, bottom, δV_b, and lateral, δV_l, surfaces of the parallelepiped form the canopy boundary δV. Trees in V are represented by cylinders with the base radius r_B and the height H. Non-dimensional scattering centres (leaves) are assumed to be uniformly distributed and spatially uncorrelated within tree crowns. The extinction coefficient takes on values $\sigma(\Omega)$ and zero within and outside the tree crowns, respectively. The centres of crown bases are scattered on δV_b according to a stationary Poisson point process of intensity d. The amount of leaf area in the tree crown is parameterized in terms of the plant LAI, L_0, defined as the total half leaf (needle) area in the tree crown normalized by the crown base area πr_B^2. In the Flakaliden research area, its value varies between 5 and 15. The canopy LAI is gL_0 where $g=1-\exp(-\pi r_B^2 d)$ is the ground covered by vegetation (Huang et al., in press). A uniform and bi-Lambertian models are assumed for the leaf normal distribution and the diffuse leaf scattering phase function, respectively (Knyazikhin et al., 2005; Ross, 1981). Leaf hemispherical reflectance and transmittance are assumed to have the same value. The stochastic radiative transfer equation is used to obtain vertical profiles of horizontally averaged 3D radiation field $I_\lambda(x,\Omega)$ (Huang et al., in press; Shabanov et al., 2000). A detailed description of the stochastic model used in our simulations can be found in Huang et al. (in press).

References

Analytical Spectral Devices (ASD), Inc. (1999). *ASD technical guide* (4th ed.). Boulder, CO, USA: ASD Inc.

Bonan, G. B., Oleson, K. W., Vertenstein, M., Levis, S., Zeng, X., Dai, Y., et al. (2002). The land surface climatology of the community land model coupled to the NCAR community climate model. *Journal of Climate*, *15*, 3123–3149.

Buermann, W., Dong, J., Zeng, X., Myneni, R. B., & Dickinson, R. E. (2001). Evaluation of the utility of satellite based vegetation leaf area index data for climate simulations. *Journal of Climate*, *14*(17), 3536–3550.

Daughtry, C. S. T., Biehl, L. L., & Ranson, K. J. (1989). A new technique to measure the spectral properties of conifer needles. *Remote Sensing of Environment*, *27*, 81–91.

Davis, A. B., & Knyazikhin, Y. (2005). A primer in three-dimensional radiative transfer. In A. Marshak & A.B. Davis (Eds.), *Three-dimensional radiative transfer in the cloudy atmosphere* (pp. 153–242). Springer-Verlag.

Dickinson, R. E, Henderson-Sellers, A., Kennedy, P. J., & Wilson, M. F. (1986). *Biosphere atmosphere transfer scheme (BATS) for the NCAR community climate model.* NCAR technical note, NCAR, TN275+STR 69 pp.

Disney, M., Lewis, P., Quaife, T., & Nichol, C. (2005). A spectral invariant approach to modeling canopy and leaf scattering. *Proc. the 9th International Symposium on Physical Measurements and Signatures in Remote Sensing (ISPMSRS), 17–19 October 2005, Beijing, China, Part 1*(pp. 318-320).

Disney, M., Lewis, P., & Saich, P. (2006). 3D modeling of forest canopy structure for remote sensing simulations in the optical and microwave domains. *Remote Sensing of Environment*, *100*, 114–132.

Huang, D., Knyazikhin, Y., Wang, W., Deering, D. W., Stenberg, P., Shabanov, N., et al. (in press). Stochastic transport theory for investigating the three-dimensional canopy structure from space measurements. *Remote Sensing of Environment*.

Kiehl, J. T., Hack, J. J., Bonan, G. B., Boville, B. A., Briegleb, B. P., Williamson, D. L., et al. (1996). *Description of the NCAR community climate model (CCM3)*. Tech. Rep. NCAR/TN-420+STR., National Center for Atmospheric Research, Boulder, CO, 152 pp. [Available from NCAR, P.O. Box 3000, Boulder, CO 80307.]

Kiehl, J. T., Hack, J. J., Bonan, G. B., Boville, B. A., Williamson, D. L., & Rasch, P. J. (1998). The National Center for Atmospheric Research community climate model: CCM3. *Journal of Climate*, *11*, 1131–1149.

Knyazikhin, Y., & Marshak, A. (2000). Mathematical aspects of BRDF modelling: Adjoint problem and Green's function. *Remote Sensing Reviews*, *18*, 263–280.

Knyazikhin, Y., Marshak, A., & Myneni, R. B. (2005). Three-dimensional radiative transfer in vegetation canopies and cloud–vegetation interaction. In A. Marshak & A.B. Davis (Eds.), *Three-dimensional radiative transfer in the cloudy atmosphere* (pp. 617–652). Springer-Verlag.

Knyazikhin, Y., Martonchik, J. V., Myneni, R. B., Diner, D. J., & Running, S. W. (1998). Synergistic algorithm for estimating vegetation canopy leaf area index and fraction of absorbed photosynthetically active radiation from MODIS and MISR data. *Journal of Geophysical Research*, *103*, 32257–32274.

Lewis, P., & Disney, M. (1998). The botanical plant modeling system (BPMS): a case study of multiple scattering in a barley canopy. *Proc. IGARSS'98, Seattle, USA*.

Lewis, P., Hillier, J., Watt, J., Andrieu, B., Fournier, C., Saich, P., et al. (2005). 3D dynamic vegetation modeling of wheat for remote sensing and inversion. *Proc. the 9th International Symposium on Physical Measurements and Signatures in Remote Sensing (ISPMSRS), 17–19 October 2005, Beijing, China, Part 1*(pp. 144-146).

Lewis, P., Saich, P., Disney, M., Andrieu, B., & Fournier, C. (2003). Modeling the radiometric response of a dynamic, 3D structural model of wheat in the optical and microwave domains. *Proc. IEEE Geoscience and Remote Sensing Symposium. IGARSS'03, 21–25 July 2003, Toulouse, Vol. 6* (3543–3545).

Li-COR. (1989). *LI-1800 portable spectroradiometer instruction manual.* Lincoln, NE, USA: Li-COR.

Marchuk, G. I., Mikhailov, G. A., Nazaraliev, M. A., Darbinjan, R. A., Kargin, B. A., & Elepov, B. S. (1980). *The Monte Carlo methods in atmospheric optics.* New York: Springer-Verlag. 208 pp.

Mesarch, M. A., Walter-Shea, E. A., Asner, G. P., Middleton, E. M., & Chan, S. S. (1999). A revised measurement methodology for conifer needles spectral optical properties: evaluating the influence of gaps between elements. *Remote Sensing of Environment*, *68*, 177−192.

Myneni, R. B., Hoffman, S., Knyazikhin, Y., Privette, J. L., Glassy, J., Tian, Y., et al. (2002). Global products of vegetation leaf area and fraction absorbed par from year one of MODIS data. *Remote Sensing of Environment*, *83*, 214−231.

Panferov, O., Knyazikhin, Y., Myneni, R. B., Szarzynski, J., Engwald, S., Schnitzler, K. G., et al. (2001). The role of canopy structure in the spectral variation of transmission and absorption of solar radiation in vegetation canopies. *IEEE Transactions on Geoscience and Remote Sensing*, *39*, 241−253.

Potter, C. S., Randerson, J. T., Field, C. B., Matson, P. A., Vitousek, P. M., Mooney, H. A., et al. (1993). Terrestrial ecosystem production: A process model based on global satellite and surface data. *Global Biogeochemical Cycles*, *7*(4), 811−841.

Raich, J. W, Rastetter, E. B, Melillo, J. M, Kicklighter, D. W, Steudler, P. A, Peterson, B. J, et al. (1991). Potential net primary productivity in South America: Application of a global model. *Ecological Applications*, *1*, 399−429.

Rautiainen, M., & Stenberg, P. (2005). Application of photon recollision probability in coniferous canopy reflectance model. *Remote Sensing of Environment*, *96*, 98−107.

Riesz, F., & Sz.-Nagy, B. (1990). *Functional analysis.* New York: Dover Publication, Inc. 504 pp.

Rochdi, N., Fernandes, R., & Chelle, M. (2006). An assessment of needles clumping within shoots when modeling radiative transfer within homogeneous canopies. *Remote Sensing of Environment*, *102*, 116−134.

Ross, J. (1981). *The radiation regime and architecture of plant stands Norwell, MA: Dr. W. Junk (pp.391).*

Running, S. W., & Hunt Jr., E. R. (1993). Generalization of a forest ecosystem process model for other biomes, BIOME-BGC, and an application for global-scale models. In J. R. Ehleringer & C. B. Field (Eds.), *Scaling physiological processes: Leaf to globe* (pp. 141−157). San Diego: Academic Press.

Saich, P., Lewis, P., Disney, M. I., van Oevelen, P., Woodhouse, I., Andrieu, B., et al. (2003). *Development of vegetation growth models for remote sensing applications*. Final report of ESA contract AO/1-3679/00/NL/NB (available from www.geog.ucl.ac.uk/~psaich/esa/fullindex.htm)

Sellers, P. J., Mintz, Y., Sud, Y. C., & Dalcher, A. (1986). A simple biosphere model (SiB) for use within general circulation. *Journal of Atmosphere Science*, *43*.

Shabanov, N. V., Knyazikhin, Y., Baret, F., & Myneni, R. B. (2000). Stochastic modeling of radiation regime in discontinuous vegetation canopies. *Remote Sensing of Environment*, *74*(1), 125−144.

Shabanov, N. V., Wang, Y., Buermann, W., Dong, J., Hoffman, S., Smith, G., et al. (2003). The effect of spatial heterogeneity in validation of the MODIS LAI and FPAR algorithm over broadleaf forests. *Remote Sensing of Environment*, *85*, 410−423.

Smolander, S., & Stenberg, P. (2005). Simple parameterizations of the radiation budget of uniform broadleaved and coniferous canopies. *Remote Sensing of Environment*, *94*, 355−363.

Tian, Y., Wang, Y., Zhang, Y., Knyazikhin, Y., Bogaert, J., & Myneni, R. B. (2003). Radiative transfer based scaling of LAI/FPAR retrievals from reflectance data of different resolutions. *Remote Sensing of Environment*, *84* (1), 143−159.

Verhoef, W. (2004). Extension of SAIL to model solar-induced canopy fluorescence spectra. *2nd International Workshop on Remote Sensing of Vegetation Fluorescence, Nov. 2004, Montreal, Canada*.

Vladimirov, V. S. (1963). *Mathematical problems in the one-velocity theory of particle transport*. Tech. Rep. AECL-1661, At. Energy of Can. Ltd., Chalk River, Ontario, 302 pp.

Wang, Y., Buermann, W., Stenberg, P., Smolander, H., Häme, T., Tian, Y., et al. (2003). A new parameterization of canopy spectral response to incident solar radiation: Case study with hyperspectral data from pine dominant forest. *Remote Sensing of Environment*, *85*, 304−315.

WWW1: *Report on Flakaliden field campaign*, Sweden, June 25–July 4, 2002. http://cybele.bu.edu/modismisr/validation/expts.html